NOVA SCHOOL OF SCIENCE & TECHNOLOGY

DEPARTMENT OF PHYSICS

DAVID HENRIQUES TRINDADE

Bachelor of Science in Biomedical Engineering

DEVELOPMENT OF A DEVICE FOR KINEMATIC AND ELECTROMYOGRAPHYIC ANALYSIS OF THE UPPER LIMB IN A CLINICAL CONTEXT

MASTER IN BIOMEDICAL ENGINEERING

NOVA University Lisbon
September, 2023

NOVA SCHOOL OF SCIENCE & TECHNOLOGY

DEPARTMENT OF PHYSICS

DEVELOPMENT OF A DEVICE FOR KINEMATIC AND ELECTROMYOGRAPHYIC ANALYSIS OF THE UPPER LIMB IN A CLINICAL CONTEXT

DAVID HENRIQUES TRINDADE

Bachelor of Science in Biomedical Engineering

Adviser: Prof. Cláudia Regina Pereira Quaresma
Assistant Professor, NOVA University Lisbon

Co-adviser: Prof. Carla Maria Quintão Pereira
Assistant Professor, NOVA University Lisbon

Examination Committee

Chair: Prof. Célia Maria Reis Henriques
Associate Professor, NOVA University Lisbon

Rapporteur: Prof. Paulo António Martins Ferreira Ribeiro
Associate Professor, NOVA University Lisbon

Adviser: Prof. Cláudia Regina Pereira Quaresma
Assistant Professor, NOVA University Lisbon

MASTER IN BIOMEDICAL ENGINEERING

NOVA University Lisbon
September, 2023

Development of a device for kinematic and electromyographyic analysis of the upper limb in a clinical context

This document was created with the (pdf/Xe/Lua)LaTeX processor and the NOVAthesis template (v6.9.5) [1].

ACKNOWLEDGEMENTS

As my academic journey comes to an end, I extend my gratitude to those who enabled my success.

First i would like to thank my advisers Cláudia Quaresma and Carla Quintão who gave me the opportunity to work in this project, and for the guidance and motivation they gave me during the development of this dissertation.

To professor Patricia Santos, thank you for your assistance with the acquisitions.

To my colleague Inês Garcia, thank you for your assistance with data processing and for always be available to clarify my questions.

To my colleague Pedro Correia, who was always available to help me and gave his opinion when I asked him.

To Ricardo Santos and Tomás Pereira of Fraunhofer, who generously invited me to their workplace and devoted their time towards my project.

I extend my gratitude to all who provided assistance in any form with this project.

To my friends, thank you for always supporting me and for the memories made through the years. A special thanks to those who assisted with the acquisitions upon my request.

Lastly, I express my deepest gratitude to my family for their unwavering support and for always believe in me. Without you, I would not be able to get where I am.

"Once we accept our limits, we go beyond them"
(Albert Einstein)

ABSTRACT

Stroke is a leading cause of disability worldwide, significantly impacting individuals ability to perform Activities of Daily Living (ADL). Therapists assess patients limb functionality through observation and personal opinion in order to develop recovery plans. However, these plans may not always align with the patient's specific needs. The examination of limb functionality using Electromiography (EMG) and kinematic parameters during ADL presents additional behavioral parameters. This allows for the development of personalized plans based on individual patient needs. Nevertheless, limited studies combine these two parameters to evaluate limb functionality during ADL, creating a knowledge gap in this area. This project aims to develop a prototype of a device capable of acquiring EMG and kinematic data, namely acceleration and angular velocity via an Inertial Measurement Unit, focusing on the shoulder complex, for use in a clinical setting. Additionally, an interface has been developed for communication and visualization of the collected data. To assess the device's performance, samples were obtained from healthy individuals performing the ADL of "Drinking water from a cup", while acquiring EMG data from the Andterior Delotoid and the raw angular velocity and acceleration. The data relating to electromyographic activity and acceleration in the X and Y axes were compared with the results obtained in a previous work, which is still under development, in which a reference device was used. The EMG graphs are quite similar, being characterized by three peaks, while those of acceleration on the X and Y axes also show similar behavior between both works. Regarding AV, it is possible to conclude that certain movements mainly affect certain axes, namely, the X axis is affected by abduction and adduction movements, Y by rotations and Z by flexion and extension movements. The results obtained allowed to conclude that the prototype is capable of collecting data, which are quite similar to those obtained with a reference device.

Keywords: Upper Limb, Activities of Daily Living, Electromyography, Inertial Measurement Unit, Angular Velocity, Acceleration

Resumo

O Acidente Vascular Cerebral é uma das principais causas de incapacidade a nível global, afetando o nível de vida das pessoas na execução de Atividades da Vida Diária (AVD). A avaliação da funcionalidade dos membros é feita por terapeutas que recorrem à observação e opinião pessoal para elaboração de planos de recuperação para os doentes. No entanto, estes planos nem sempre correspondem às necessidades específicas dos pacientes. O estudo da funcionalidade do membro com recurso a Eletromiografia (EMG) e parâmetros cinemáticos na execução de AVD fornece mais parâmetros sobre o comportamento deste, sendo então possível estabelecer planos mais personalizados de acordo com as necessidades de cada paciente. Contudo, são poucos os estudos em que estes dois parâmetros são utilizados para avaliar a funcionalidade do membro na execução de AVD, pelo que há uma lacuna neste aspeto. Este projeto tem o objetivo de desenvolver um protótipo de um dispositivo capaz de recolher dados EMG e cinemáticos do complexo do ombro, nomeadamente aceleração e velocidade angular, com recurso a uma Unidade de Medição Inercial, com o objetivo de ser aplicado num contexto clínico. Uma interface também foi criada para comunicação e visualização dos dados recolhidos pelo dispositivo. De modo a avaliar o desempenho do dispositivo, foram feitas recolhas em indivíduos saudáveis da AVD "Beber água de um copo", adquirindo dados de EMG do Deltóide Anterior e a velocidade angular e aceleração. Os dados relativos à àtividade eletromiográfica e à aceleração nos eixos X e Y foram comparados com os resultados obtidos num trabalho anterior, que ainda se encontra em desenvolvimento, no qual foi utilizado um dispositivo de referência. Os gráficos de EMG são bastante semelhantes, sendo este caracterizado por três picos, enquanto os da aceleração nos eixos X e Y também apresentam um comportamento semelhante entre ambos os trabalhos. Relativamente à VA é possível concluir que certos movimentos afetam maioritariamente certos eixos, nomeadamente, eixo do X é afetado pelos movimentos de abdução e adução, Y pelas rotações e Z pelos movimentos de flexão e extensão. Os resultados obtidos permitiram concluir que o protótipo é capaz de recolher dados, sendo estes bastante semelhantes aos obtidos com um dispositivo de referência.

Palavras-chave: Membro Superior, Atividades da Vida Diária, Eletromiografia, Unidade de Medição Inercial, Velocidade Angular, Aceleração

Contents

List of Figures

List of Tables

ABBREVIATIONS

ACC Acceleration
AD Anterior Deltoid
ADL Activities of the Daily Living
AP Action Potential
ARAT Action Research Arm Test
AV Angular Velocity

EMG Electromiograpy

IMU Inertial Measurement Unit

MAF Moving Average Filter
MU Motor Unit

OS Optoelectronic Systems

ROM Range of Motion

SD Standard Deviation
SR Sarcoplasmic Reticulum

UL Upper Limb

CHAPTER 1

INTRODUCTION

1.1 Motivation

The Upper Limb (UL) is a fundamental structure of the human body, with considerable Range of Motion (ROM) and significant impact on the ability to perform Activities of the Daily Living (ADL) [2].

Neurological disorders, such as stroke, can affect the mobility of the UL. Stroke is defined as a clinical syndrome characterized by the rapid development of focal or global disturbance in cerebral function lasting for more than 24 hours or leading to death due to a presumed vascular cause [3]. Globally, 16 million people have a stroke each year and it is the 2nd highest cause of death and the 3rd leading cause of incapacity worldwide, with significant economic consequences, with a total cost of 64 billion euros per year [3], [4].

Almost 80% of stroke survivors experience mobility impairments in the UL, with up to 50% still reporting motion issues after six months [5]. The loss of UL functionality is one of the major consequences after stroke, resulting in challenges for patients to carry out their ADL [3]. Compensatory movements may arise from this, and while effective with appropriate training, they may result in adverse effects such as pain, limited motion range, and inadequate recovery over an extended period [6], [7].

The evaluation of the functionality of the limb is made by therapists through qualitative scales, which may be influenced by their opinion and experience [8]–[10]. Therefore, these scales may not accurately represent the optimal assessment for an individual patient, highlighting the need for additional information to provide a tailored treatment [11].

A suitable approach to evaluate the kinetic and kinematic parameters of the UL during ADL is using Optoelectronic Systems (OS) and Inertial Measurement Unit (IMU) [10]. However, most studies focus on the lower limb, since it is easier to establish a motor pattern [12]. In the studies concerning UL kinematic parameters, functional capacity of the limb in healthy

people performing ADL is assessed, with limited information on these parameters in stroke patients [12], [13]. The use of Electromiograpy (EMG) to measure muscle activation is not a common practice, so there is a gap in this regard, to better understand the patterns of muscle activation while performing ADL.

This dissertation follows another study, still in development, in which a protocol was developed for collecting kinematic and electromyographic data from the shoulder complex during the execution of ADL in a healthy population, to understand the typical pattern of the movement. The device utilised in the study is validated and available on the market. A normative base was also developed to compare the data between healthy and pathological population [14].

Studying UL muscle activity and combining it with kinematic data allows a comprehensive understanding about the functionality of the limb. The movements performed during ADL are complex, requiring various actions to perform them. However, few studies have combined these type of data during ADL, resulting in a knowledge gap regarding the movements necessary for basic daily tasks while collecting EMG and kinematic parameters. With this information, a therapist's analysis could be more complete, because they would not rely only on observation and recovery plans for the patients would be much more personalized, according the needs of each.

1.2 Objectives

The goal of this dissertation is to develop a prototype, for a portable low cost device incorporated with inertial and EMG sensors, able to define and analyse the movement patterns of the UL, with a particular emphasis on the shoulder, in a clinical environment. Additionally, an interface is also intended to be developed, to allow the control of the device and visualize the data obtained from it.

With the development and validation of this device in healthy individuals, its use is expected in stroke patients, as a tool for healthcare professionals to elaborate rehabilitation plans.

During the realization of this project, the following tasks were performed:

1. Familiarization with the previous work for the construction of the normative base;
2. Definition of requirements and specifications of the device to be developed, in partnership with doctoral student Patricia Santos [15];
3. Definition of device design and construction, also together with Patricia Santos;
4. Development of an interface to visualize the data obtained from the device.
5. Elaboration of tests in a laboratory context in a sample of healthy individuals with the device developed;
6. Comparison of the data collected from the device with data collected by Garcia;

The research work described in this dissertation was carried out in accordance with the norms established in the ethics code of Universidade Nova de Lisboa. The work described and the material presented in this dissertation, with the exceptions clearly indicated, constitute original work carried out by the author.

CHAPTER 2

THEORETICAL CONCEPTS

In this chapter the theoretical concepts necessary to understand this thesis will be explained. The anatomy of the shoulder and the concepts of EMG, OS and IMU will be covered.

2.1 Shoulder Anatomy

The shoulder is a complex structure and it is the most mobile part of the body [16]. Due to its mobility, it can deteriorate over time, causing wear and tear on the joints, which can lead to dislocations and injuries, as well as being affected by neurological conditions such as stroke or Parkinson's disease [7], [17].

Before diving into the shoulder anatomy, it is important to understand the reference planes for human movement (Figure 2.1). The sagittal plane divides the body into left and right sides, conditions the notions of medial and lateral, and is where flexion and extension movements occur; the frontal/coronal plane, divides the body into anterior and posterior portions, and is where abduction and adduction movements occur; the axial plane, divides the body into upper and lower portions and the movements that happen here are internal and external rotation [18].

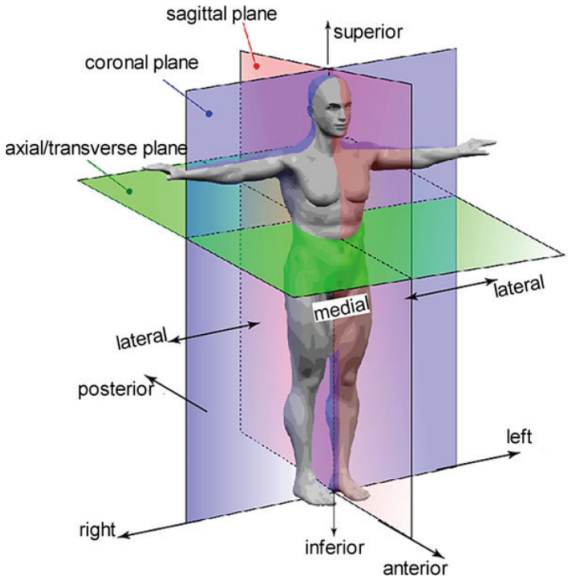

Figure 2.1: Anatomical planes. Adapted from [19]

2.1.1 Osteology of the Shoulder

The shoulder is made up by three bones, presented in the Figure 2.2: the clavicle, the scapula and the humerus [17].

The clavicle is a superficial and horizontal bone, with an S-shape and has two curvatures, one medial with posterior concavity and the other lateral with anterior concavity. It articulates with the sternum and with the scapula, connecting the shoulder to the trunk [17], [18].

The scapula is a flat, triangular bone located in the posterior part of the shoulder [17]. It has two faces, one posterior and one anterior, the latter being concave, three edges, medial, superior and lateral, and three angles, superior, inferior and lateral. It articulates with the clavicle and with the humerus in the glenoid fossa of the anterior surface [18].

The humerus is the largest bone in the UL, but only its proximal portion, consisting of the humeral head, greater and less tuberosities, humeral neck and bicipital groove, are part of the shoulder complex [17], [20]. Its head consists of a third of a sphere and articulates with the scapula, as mentioned above [18].

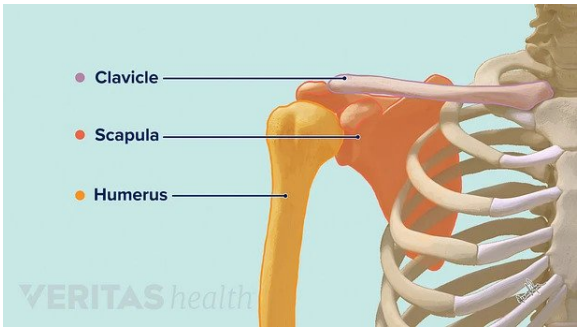

Figure 2.2: Shoulder bones. Adapted from [21]

2.1.2 Arthrology of the Shoulder

The shoulder is made up of four joints, as can be seen in the Figure 2.3: the acromioclavicular, glenohumeral, sternoclavicular and scapulothoracic joints [17].

The acromioclavicular joint articulates the lateral end of the clavicle with the acromion, attaching the scapula to the thorax, giving this bone greater freedom of movements. It also provides stability to the shoulder. Under normal conditions, it allows only gliding movement. This joint is surrounded by a capsule and lined by a synovial membrane. Between the bony parts lies an intra-articular cartilaginous disc. Three ligaments stabilize this joint: acromioclavicular, coracoclavicular and coracoacromial ligaments [22].

The glenohumeral joint is a ball-and-socket joint that connects the rounded head of the humerus with the glenoid fossa. Its spherical shape allows the shoulder to move in a variety of planes and angles (flexion, extension, internal and external rotation, adduction and abduction), making it the most mobile joint in the human body. There are important structures in the joint such as the synovial fluid (reduces friction between the articular surfaces), bursae (the most important are subacromial, subcoracoid and subscapular, which act as a cushion between the joint structures) and ligaments (glenohumeral, coracoclavicular and coracohumeral) [23].

The sternoclavicular joint connects the axial skeleton to the UL, articulating the clavicle to the sternum. The surfaces of the joint are separated by a fibrocartilaginous articular disc that allows mobility in the anteroposterior and vertical axes. The ligaments that stabilize the SC joint are the posterior, anterior, costoclavicular and interclavicular ligaments [24].

The scapulothoracic joint is the articulation between the scapula and the thorax. It allows the elevation and depression of the shoulder to change the plane of motion [17].

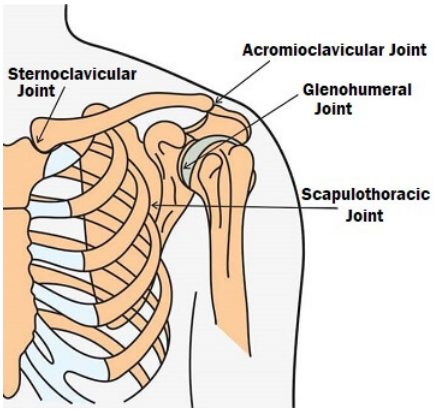

Figure 2.3: Shoulder joints. Adapted from [25]

2.1.3 Miology of the Shouder

The muscles that allow the the shoulder to move are presented next and can be seen in the Figure 2.4:

- **Deltoid** - big muscle with a triangular shape that originates from the scapula and the lateral third of the clavicle and inserts into the deltoid tuberosity of the humerus. It is

formed by three fibers: anterior are responsible for flexion and protraction of the shoulder, and medial rotation and abduction of the humerus, middle abduct the humerus and does shoulder flexion and extension, and posterior are responsible for the extension, external rotation and abduction of the humerus and extension of the shoulder [18], [26].

- **Teres Major** - extends from the scapula to the humerus and inserts into the infraspinatus fossa. Adducts, extends and medially rotates the arm and does shoulder extension [18], [26].

- **Rotator Cuff**

  - Supraspinatus - has a triangular pyramidal shape and inserts into the supraspinatus fossa, in the scapula, and in the superior aspect of the lesser tubercle of the humerus. Assists in abduction of the arm [18], [26].
  - Infraspinatus - has a flat triangular shape and inserts in the infraspinatus fossa and in the middle facet of the lesser tubercle of the humerus. Rotates the arm laterally [18], [26].
  - Teres minor - it is a cylindrical muscle and inserts into the infraspinatus fossa and in the inferior facet of the lesser tubercle of the humerus. Rotates laterally and adducts the arm [18], [26].
  - Subscapularis - has a triangular shape and inserts in the subscapular fossa and in the greater tubercule of the humerus. Adducts and rotates the arm medially [18], [26].

- **Trapezius** - arises on the superior aspect of the nuchal line and inserts into the clavicle, acromion and scapula. It is formed by three fibers: the superior elevates the scapula and rotates it during the arm abduction, the middle retracts the scapula, and the inferior pulls the scapula down [18], [26].

- **Latissimus Dorsi** - originates from the spine, iliac crest, thoracolumbar fascia, and inferior third and fourth ribs and inserts into the intertubercular groove of humerus. Performs adduction, external rotation and extension of the arm and shoulder extension [18], [26].

- **Levator scapulae** - arises from vertebrae C_1 and C_4 and inserts into the scapula. Elevates the scapula [18], [26].

- **Rhomboid Major** - arises from vertebrae T_2 and T_5 and inserts into the scapula. Retracts and rotates the scapula [18], [26].

- **Rhomboid Minor** - originates at vertebrae C_7 and T_1 and inserts into the scapula. Retracts and rotates the scapula [18], [26].

- **Serratus Anterior** - it is located against the lateral wall of the thorax. This muscle has 3 portions: superior, that inserts in the superior angle of the scapula and on the first and second ribs; middle, inserts in the middle of the scapula and on the second, third and fourth ribs; inferior, inserts in inferior angle of the scapula and between the fifth and tenth ribs. Does shoulder protraction and rotates the scapula [18], [26].

- **Pectoralis Major** - it is the most superficial of the anterior muscles of the shoulder. Has 4 fascicles: the clavicular fascicle, which inserts into the medial two-thirds of the anterior border of the clavicle; the sternal fascicle, which inserts into the anterior surface of the sternum; the abdominal fascicle, which inserts into the anterior layer of the sheath of the rectus abdominis; and the chondrocostal fascicle which inserts into the anterior surface of the first six ribs and their respective costal cartilages. Protracts the shoulder, flexes the clavicle, adducts the arm and sternum and medially rotates the arm [18], [26].

- **Pectoralis Minor** - it is located posteriorly to the pectoralis major and inserts into the superior margin and external face of the third, fourth and fifth ribs and in the medial margin of the coracoid process. Performs shoulder depression [18], [26].

- **Subclavius** - small cylindrical muscle that extends from the clavicle to insert into the first rib and first costal cartilage. Stabilizes and makes the depression of the clavicle [18], [26].

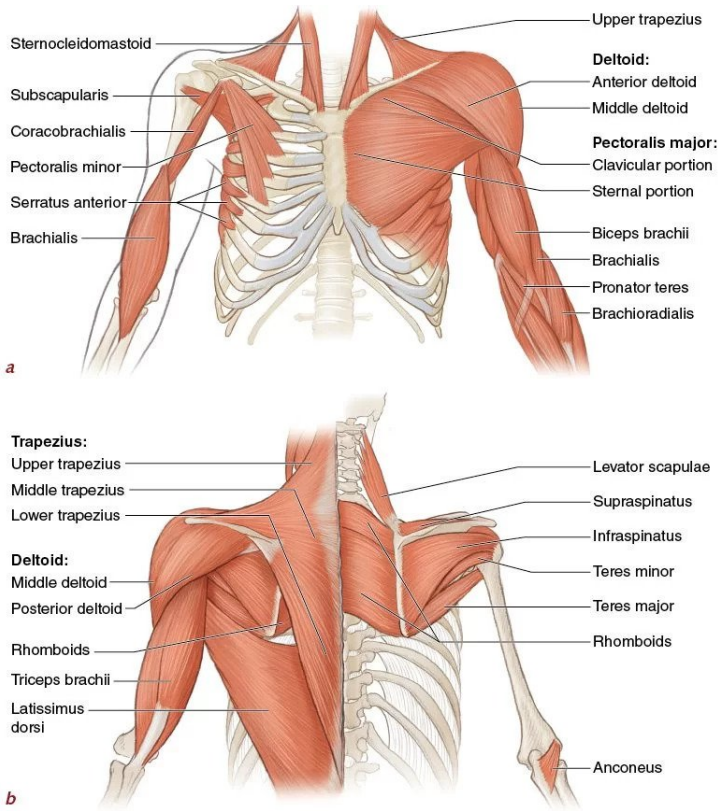

Figure 2.4: Muscles of the shoulder. A: Anterior view. B: Posterior View Adapted from [27]

2.2 Electromyography

The electromyographic signals represent the neuromuscular activity of a given muscle and the observed signal corresponds to the electrical activity of a muscle contraction [28].

Skeletal muscle is made up of muscle fibers, in which myofibrils made up of thick (myosin) and thin (actin, tropomyosin and troponin) filaments are arranged in parallel and longitudinally in smaller units called sarcomeres [29].

Muscle contraction occurs when an Action Potential (AP) causes the myocyte membrane to depolarize. Muscle cells have a resting membrane potential of -90 mV due to ion pumps and channels, and neurotransmitter receptors. When acetylcholine binds to receptors at the neuromuscular junction, it causes depolarization of the cells and the beginning of the AP. The AP spreads from the sarcolema into the t-tubules, causing changes in the voltage of the dihydropyridine receptors. These receptors are near the ryanodine receptors of the Sarcoplasmic Reticulum (SR), and their opening results in the release of stored calcium into the cytoplasm, where it binds with troponin C, changing the conformation of tropomyosin, causing myosin to bind to actin (cross-bridge). Calcium is pumped back into the SR, to restore the resting concentration gradients [28], [30].

The AP is the main component of the EMG signal. The characteristics of the signal depend on the dimensions of the muscle fiber, the conduction velocity, and the relative position of the fiber with respect to the electrode that acquires the signal [28].

A group of muscle fibers innervated by a single nerve is called a Motor Unit (MU). The AP of a MU is the sum of the AP's of the contractions of the muscle fibers of a MU. The voltage detected by the sensors represents the sum of the activity of all the MU's. The MU's closer to the electrode are more easily detected, causing attenuation and noise in the signals from the more distant MU's. The more MU's are recruited, the more intense the contraction and the greater the amplitude of the signal [28].

The signal collected from the electrodes is called the raw EMG signal (Figure 2.5). When the muscle is relaxed, the signal has practically no activity. In the moments of contraction, spikes with random shape appear in the signal, meaning that one raw recording can not be reproduced in exact shape. The set of recruited MU's constantly changes and the signal contains the information of all MU's involved in muscle contraction. If more MU's are recruited, the signal will be stronger. By applying smoothing algorithms, the non reproducible contents of the signal are eliminated or minimized [31].

The EMG signal can be affected by various factors, such as [31]:

- Tissue characteristics: the electrical conductivity of the body can change due to tissue type, thickness, physiological changes and temperature.

- Physiological crosstalk: muscles other than those being analyzed, may be represented in the EMG signal and ECG spikes can appear when recording EMG activity from upper trunk and shoulder muscles.

- Changes in geometry between muscle belly and electrode: changes in the distance between the signal origin and electrodes will affect the output of the signal.

- External noise: voltage or electromagentic sources can cause noise in the signal, due to incorrect grounding.

- Electrodes and amplifiers: the quality and placement of the electrodes and internal amplifier noise will affect the signal.

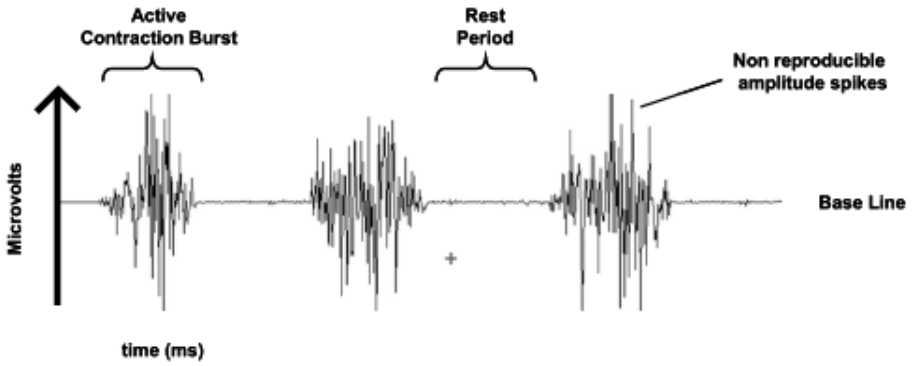

Figure 2.5: Raw EMG signal. Adapted from [31]

The acquisition of EMG can be done using surface electrodes (acquire signals from multiple MU's and can be dry, in which the electrode is placed directly in contact with the skin, or wet, using some type of gel between the skin and the electrode) or needle electrodes (acquire a signal from only a single muscle fiber with high precision, but are invasive, so they are rarely used) [28].

Different steps can be taken in order to process the raw EMG signal [31]:

- Removal of the signal average, if this suffers from baseline offset.

- Rectification of the raw signal, to convert the negative values into positive ones.

- Smoothing of the signal, by applying Moving Average Filter (MAF) or root mean square. These methods use a time window to smooth the signal, and a smaller window preserves the signal more, while a larger window smooths the signal more, but may cause a phase shift in the smoothed signal.

- The use of filters other than smoothing filters, like a low-pass filter at 6 Hz can be used to create a linear envelope EMG, or a high-pass filter at 20-25 Hz can reduce wire movement artifacts.

- Amplitude normalization, which be done to the mean or to the maximum peak value.

- Removal of ECG artifacts.

Various parameters can be analyzed in an EMG signal, such as peak-to-peak amplitude, mean amplitude, shape of the signal, activity duration, phase, Fast Fourier Transform to understand the frequencies of the signal, or signal-to-noise ratio [31].

In biomechanics, EMG can have several applications such as detection of muscle activation moments, relationship between signal strength and muscle contraction, and monitoring of fatigue levels. It can also be used in other areas such as research, rehabilitation, sports performance and studies on working conditions [28].

2.3 Optoelectronic Systems and Inertial Measurement Units

Optoelectronic Systems are considered to be the gold standard method for kinematic analysis due to their high accuracy and reliability (Figure 2.6) [10]. By placing retro-reflective markers in the desired structures to be analyzed, it is possible to obtain the absolute position of it through multiple video cameras, allowing an in vivo three dimensional analysis of the different joints through non-invasive methods [10], [32]. Makers can be passive or active, i.e., they are covered with a reflective material that reflects infrared light or they emit infrared light, respectively [33]. Although these systems have good reliability, their application in clinical facilities is almost impossible due to their high cost, difficult transportation, large setup volume, high level of technical expertise and lengthy calibration [10], [34].

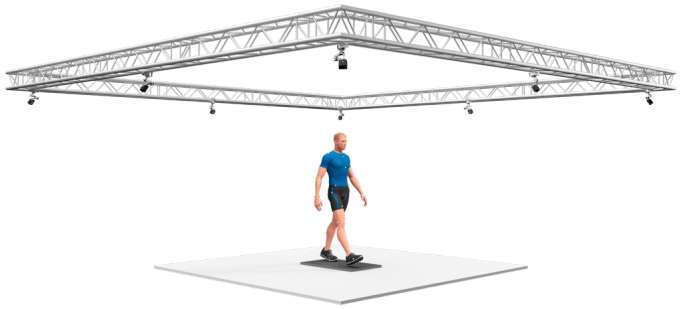

Figure 2.6: Optoelectronic System. A set of various cameras are placed surrounding the person to analyze the movement performed. Adapted from [35]

Another way to evaluate kinematic parameters is through IMU. Due to their low cost, small size, low power consumption, high availability, portability, and capability to obtain data in real time, they are a viable option for kinematic analysis in a clinical setting [34], [36], [37]. These sensors consist of accelerometers and gyroscopes that measure linear Acceleration (ACC) (with the gravitational component) and Angular Velocity (AV), respectively [38], [39]. A magnetometer can be added to the IMU to measure the local magnetic field, and these sensors are called MARG (Magnetic, Angular Rate and Gravity) [39].

It is possible to obtain IMU orientation (yaw, pitch and roll) through sensor fusion techniques, such as the Kalman or Madgwick filter [39]. By combining the accelerometer and gyroscope sensors, they complement each other and it is possible to determine orientation [40]. The gyroscope tends to drift over time, which means its measurements are more accurate for short periods of time. The accelerometer, on the other hand, does not obtain orientation,

only inclination, is more accurate over long periods of time, fails to provide information about yaw axis when the sensor frame is aligned with the Earth frame and can suffer from noise [40]–[43]. Adding a magnetometer solves the problem of gyroscope drift, which increases the accuracy of orientation estimation, because it is affected not only by the direction of gravity but also by the Earth's magnetic field [39], [40].

Chapter 3

State of the art

In this section, studies on the biomechanical assessment of the UL during ADL performance using OS and IMU are presented. Some studies also incorporate EMG.

3.1 Biomechanical and physiological evaluation methods of the Upper Limb

3.1.1 Qualitative scales

A first approach to assess the level of functionality of the UL involves the completion of questionnaires to evaluate the patient's performance in executing certain tasks, so that it is possible to establish a rehabilitation plan. These assessments are used in a conventional context and follow the guidelines of the World Health Organization, according to the International Classification of Functioning, Disability and Health [44], [45].

There are different tests to evaluate the functionality of the UL, but the most common ones are [13]:

- **Action Research Arm Test (ARAT)** - consists of nineteen activities involving grasping, griping, pinching, and gross arm movements. The performance of the movements is evaluated on a scale ranging from 0 (no movement) to 3 (movement performed normally) [46].

- **Fugl-Meyer** - scale that assesses different activities for different parts of the body in stroke patients. It has five domains: motor function, sensory function, balance, joint range of motion, and joint pain [47].

3.1.2 Kinematic Studies of the Upper Limb while executing Activities of the Daily Living in healthy people and stroke patients

The kinematics of the UL are mainly studied using OS, so that it is possible to evaluate and describe the movements performed in 3D [10].

Gates et al. studied the ROM of the entire upper body, to better understand the UL movements in certain tasks in a sample of healthy individuals. Markers were placed in the trunk, pelvis, upper arm, forearm, hand, lateral humeral epicondyles and acromial process. The angles used for the shoulder was the thoracohumeral angle, which represents the movement of the humerus in relation to the trunk, and the results for the different activities are presented below [12]:

- **Perineal care**: peak movement of the humerus elevation plane was 105º for the contralateral limb and 61º and -46º for the ipsilateral limb, anterior and posterior respectively, humerus elevation of 63º for the contralateral limb and 55º for the ipsilateral limb, internal rotation of the humerus of 3º for the contralateral limb and 65º for the ipsilateral limb, external rotation of -36º for the contralateral limb and -25º for the ipsilateral limb.

- **Deodorant**: peak humeral elevation plane motion was 100º for the ipsilateral limb and 65º for the contralateral limb, humeral elevation of 107º for the contralateral limb and 55º for the ipsilateral limb, internal rotation of the humerus for the ipsilateral limb contralateral limb of 12º and 13º for the ipsilateral limb, external rotation of -37º for the contralateral limb and -39º for the ipsilateral limb.

- **Box off shelf**: peak motion plane elevation of the humerus was 90º at fixed height and 86° at head level, humerus elevation was 108º at head level and 86º at fixed height, humerus internal rotation was 23º at fixed height and 4º at head level, external rotation was -55º at fixed height and -48º at head level.

- **Donning and zipping pants**: peak plane motion humerus elevation was 84º in front of the body and -57º behind the body, humerus elevation 51º, humerus internal rotation 79º, external rotation -20º.

- **Drinking from a cup**: peak plane motion humerus elevation was 81º anterior to the body, humerus elevation 71º, humerus external rotation -53º.

- **Can off shelf**: peak motion plane humeral elevation was 78º at fixed height and 72º at head level, humeral elevation was 105º at head level and 86º at fixed height, external rotation was -51º at fixed height and -46º at head level.

- **Hand to back pocket**: peak motion plane humeral elevation was 80º anterior to the body and -65º posterior to the body, humeral elevation was 80º, humeral internal rotation was 79º, external rotation was -53º.

- **Box off ground**: peak motion plane humerus elevation was 75º anterior to the body, humerus elevation 69º, humerus internal rotation 3º, external rotation -45º.

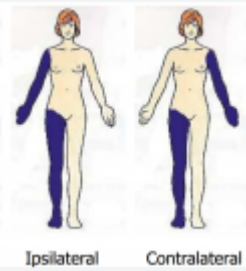

Figure 3.1: Ipsilateral and Contraleteral sides. Adapted from [48]

Magermans et al. also studied the motion of the UL but with a different approach. Instead of using the thoracohumeral angle, he studied the ROM of the glenohumeral joint directly and the results obtained were similar to those obtained by *Gates et al* [2].

Kim et al. compared the kinematic differences between stroke patients and a control group during the task of drinking water from a cup. The movement was divided into different phases due to its complexity and to facilitate the analysis. Data were collected using OS and the movement time, phase ratio, joint angles and AV were calculated. The movement time was higher in stroke patients, especially in the transportation of the cup to the mouth. Different joints were analyzed , but regarding the shoulder, abduction angles were greater in stroke patients, during forward transportation to the return phase. Shoulder flexion was also different between the two groups during cup transportation and drinking, but external and internal rotation were not. The AV of shoulder flexion was smaller in the stroke patients during forward transportation. They also had difficulties when returning the cup to its original spot. This occurs because the muscles of stroke survivors are weakened, making it difficult to perform the movement due to the lack of muscle coordination. This study helped to better understand the problems stroke patients have in performing ADL and also compared them with a healthy population to understand the differences between these two groups [49].

Different studies have compared the data obtained from IMU with OS or goniometers, with the main objective to validate these sensors, and the results have been very positive. There are many studies focused on the lower limb, because it is easier to evaluate its kinematic and kinetic parameters [50]–[53]. Regarding the UL, there are also a few studies, where the kinematic and kinetic parameters are evaluated using IMU, but in many cases, the movements performed are quite simple, and do not represent the complexity of ADL [54]–[57].

Nam et al. proposed a novel parameter to assess UL impairment using IMU in stroke patients. The tests were performed in healthy subjects and stroke patients while performing ADL and compared with the results of ARAT. The sensors were placed in the upper extremities to obtain data from the major joints of the UL (performance time, average and maximum motion segment size for position and angle). The results obtained indicate that the use of these sensors may be a good approach to evaluate the impairment of the UL, because it combines

the data from the IMU of both activities set to give a full understanding of the functionality of the UL [58].

Kirking et al. measured shoulder joint angles with IMU's in a sample of people outside the laboratory environment, with the goal of characterizing shoulder kinematics during ADL, comparing activities simulated in the laboratory with more common daily activities, and providing information for clinical evaluation of shoulders and their treatment. Results were compared to a robotic arm [59].

Held et al. studied the complementarity between upper limb recovery post stroke measured with standard clinical assessments and ADL recorded with IMU. The sensors were placed in a full body suit and data were recorded at different stages of the recovery process in a clinical setting and at home. The results obtained showed that it is possible to use IMU outside the laboratory or clinical environment to obtain more detailed data about a patient's recovery and behaviour at home. However, there were some problems with the data collection and it is necessary to improve the technology, due to loss of sensor data and sensor drift [60].

There are a few studies where kinematic, kinetic and electromyographic data were collected simultaneously. The addition of EMG allows to understand the muscle contraction patterns during the different movements, giving a more detailed understanding of how the movements are performed. The majority of studies use OS and the movements performed are quite simple and do not represent the complexity of ADL [61]–[64].

Ricci et al. studied the movement patterns of the UL and muscle contractions during a simple ADL, of pouring water into a cup, in a healthy population to better understand the adaptations of control strategies during a basic ADL. Movement was captured using OS and EMG activity was collected from various muscles of the shoulder, arm, forearm and hand. With this study, it was possible to determine which muscles have a greater influence in the different phases of the movement and also to understand the ROM of the different joints of the UL, in a healthy population, so when this is applied to people with impaired motor function, it will help to determine if there is a compensatory movement and apply the best possible treatment [65].

Repnik et al. combined both IMU and EMG to analyze the movement patterns of the upper limb while performing tasks of the ARAT test in stroke patients and healthy subjects. The parameters obtained were movement time, movement smoothness, similarity of hand trajectories, trunk stability, and finger and wrist muscle activity. With this, it was possible to analyze the movement patterns in the different phases of the movement to obtain a more detailed quantification of the limitations in the movement of the arm. However, the ARAT test does not represent the complexity of some ADL movements [66].

Considering the aforementioned studies, the use of EMG and kinematic data to evaluate UL functionality during ADL is not a common practice. Therefore, it is important to develop methods and a system that is able to evaluate the performance of different movements that are important for the basic daily activities, so that a more complete analysis can be made in order to provide recovery plans that are more focused on the problems of each patient.

Chapter 4

Materials and Methods

This chapter describes the means used to achieve the final objective, more specifically, the questionnaires used to characterize the samples, the acquisition system, the algorithms used to program the microcontroller and to develop the interface, the protocol used for data acquisition and the processing of the signals. This study was approved by the Ethics Committee of FCT NOVA.

4.1 Sample Characterization Questionnaires

Prior to each acquisition, participants were required to read and sign an informed consent form and complete a questionnaire (Appendix A). The purpose of the questionnaires was to collect information about the subjects that could be relevant to this study. The information collected were:

- Biomechanical characteristics: age, date of birth, height and weight;
- Gender;
- Dominant limb;
- Practice of physical activity (frequency, sports practiced and if the sports involve a great activity of the UL).

4.2 Acquisition System

The objective of this work is to develop a prototype of a low-cost device capable of acquiring electromyographic and kinematic data of the shoulder complex. The system had to be able to

collect EMG data of six different muscles and kinematic parameters, have small dimensions, be portable, have low power consumption and communicate via wireless.

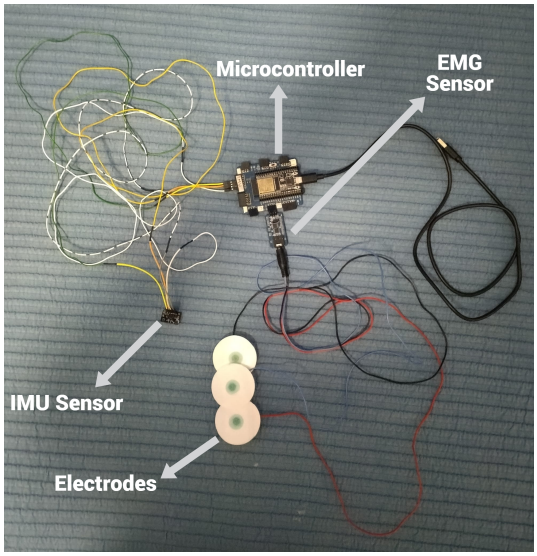

Figure 4.1: Prototype developed with the different components: IMU sensor, micorcontroller, EMG sensor and electrodes

Data were collected using the hardware developed by WallySci (Neuriot Technologies LLP, India). The system developed by this company is specifically designed to collect physiological and kinematic data. This kit consists of a microcontroller (ESP32-WROOM-32D, Figure C.1), which has the ability to work wirelessly through Bluetooth or WiFi, is attached to a board that is packed with 10 GPIO, has 6 analog inputs of 12 bits and 2 analog outputs of 8 bits, is able to collect data at a sampling rate interval from 1 to 2000 Hz and supports various communication protocols including SPI, I2C and UART. The kit also includes four sensor modules (1 EMG, 2 ECG/EEG and 1 IMU; only the EMG and IMU sensors were used), electrode cables, USB cable and a set of adhesive electrodes. The EMG module has a gain of 1920, the signal amplitude varies between ±0.8 mV, a frequency band between 50 and 2500 Hz, a CMRR of 90 dB, an input impedance of 0.8 GOhm, a power supply between 2.7 and 5 volts, and is compatible with Arduino (Figures C.2 and C.3) [67].

The EMG sensor has two acquisition options, raw and integrated. The integrated option was used because the raw data had too much noise. Integrated EMG is defined as the area under the curve of the rectified EMG signal, which is one of the standard amplitude parameters to represent EMG signal characteristics. This parameter facilitates the visualization of muscle activation [68].

Due to a malfunction of the IMU sensor from the WallySci kit, another sensor was used, a MPU6050 (DFRobot, China). The sensor has a 3D accelerometer and a 3D gyroscope, that are used to collect the raw ACC with the gravity component and the raw AV. Scales need to be defined for the IMU, so it was chosen a scale of ±2g for the ACC and ±250 rad/s for the AV. The communication between the board and the sensor was made through I2C protocol (Figure C.4).

The board was powered by the USB cable, that could be connected to a charger or a laptop.

4.3 Algorithms used

4.3.1 Microcontroller

For the microcontroller, a C++ code available on a Github page from the user Kriswiner was used, which works for the MPU6050 using the Madgwick filter for sensor fusion [69]. Only the raw accelerometer and gyroscope data were recorded, but for future work, it is necessary a code that includes the orientation of the sensor. Therefore, different codes with different fusion techniques were tested, and the Madgwick filter was the one that seemed to perform better. The others included the Complementary, Kalman and Mahony filters and also the DMP (Digital Motion Process), which is a microchip built into the MPU6050 that does the sensor fusion.

For the code to work properly, some libraries had to be added, such as the Wire, which allows the I2C communication between the microcontroller and the MPU6050, the Madgwick-AHRS, which is necessary for the Madgwick filter, and the BluetoothSerial, which activates the Bluetooth module of the ESP32.

First, the protocols to establish the I2C communication, the baud rate of 115200 and the serial Bluetooth communication are defined. Then, some tests are made to verify that the MPU6050 is working correctly and the bias and offsets are calculated, to do the calibration of the sensor.

To acquire data, there are three main functions that work together: 'loop', 'Ler_teclado' and 'Aquisicao'.

The 'loop' function constantly checks if there is data available to read from the Bluetooth serial communication, and if there is, it calls the 'Ler_teclado' function to process the information received via Bluetooth. The 'loop' function also has a condition to check the 'Aquisicao' function every 0.5 milliseconds, to ensure that data is acquired at regular intervals.

The 'Ler_teclado' function processes the messages that are received via Bluetooth. If the received message is '1', it turns the boolean 'executa' to true (its initial state is equal to false), which gives a command to the 'Aquisicao' function to start acquiring data. If the received message is '0', the boolean 'executa' is set back to false and the acquisition is stopped.

The 'Aquisicao' function first checks if the boolean 'executa' is true and if it is, it starts collecting and sending data via Bluetooth, through serial communication. The raw readings from the accelerometer and gyroscope are retrieved from the MPU6050 and they are converted into the scales mentioned previously. The quaternions are also calculated and used to determine yaw , pith and roll, which will be explained later. Conditions have been created to check the current time and every 10 milliseconds a message with the IMU data is sent via Bluetooth and every millisecond the EMG data is sent in a different message via Bluetooth.

To obtain orientation using the Madgwick filter, it is necessary to obtain the quaternions. These can be defined as a four-dimensional vector ($q0$, $q1$,$q2$ and $q3$ represent real values and i, j and k the imaginary part) that represents rotations in 3D space (Equation 4.1). Unlike the Euler angles, quaternions represent orientation differently and more efficiently, avoiding

gimbal lock problems and providing seamless interpolation between rotations [39], [70].

$$q = q_0 + q_1 i + q_2 j + q_3 k \tag{4.1}$$

To calculate the quaternions a function was created in the code. First, the accelerometer data is normalized, to form a unit vector representing the direction of the gravity vector in the sensor frame [69]. Then, the objective function and jacobian elements are computed and used in the gradient descent step to minimize the error between the estimated and measured accelerometer directions [69]. After obtaining the gradient descent, the resulting vector is normalized to ensure it is a unit vector and is used to estimate the gyroscope biases, which are then estimated and adjusted based on the time step and a bias correction factor [69]. The biases are then removed from the raw gyroscope data to reduce the effects of the drift [69]. The derivative of the quaternion components is calculated based on the adjusted gyroscope readings, which are then integrated to update the quaternion components over time [69]. The updated quaternion is normalized to ensure that it represents a valid orientation in 3D space [69]. After obtaining the quaternion vector, it is possible to obtain the yaw, pitch and roll values, by applying the respective formulas represented in the Equations 4.2, 4.3 and 4.4. The yaw, pitch and roll are in radians, and to convert them to degrees, it is just necessary to multiply the value by 180 and then, divide it by π [39], [69].

$$yaw = atan2(2.0 * (q[1] * q[2] + q[0] * q[3]), q[0]^2 + q[1]^2 - q[2]^2 - q[3]^2) \tag{4.2}$$

$$pitch = -asin(2.0 * (q[1] * q[3] - q[0] * q[2])) \tag{4.3}$$

$$roll = atan2(2.0 * (q[0] * q[1] + q[2] * q[3]), q[0]^2 - q[1]^2 - q[2]^2 + q[3]^2) \tag{4.4}$$

4.3.2 Interface

A simple and easy-to-use Python Interface was developed for communication between the laptop and the board, and for data visualization. The necessary requirements for the interface were as follows:

- A button to connect the microcontroller to the application and a way to ensure that the connection has been established.
- A button to start and another to stop data acquisition.
- The possibility to select the channels related to the data we want to visualize.
- A part aimed at filling in some patient data.
- Allows real-time visualization of different data collected in graphs, with the corresponding units and each graph in a different color.

When the Interface is opened, it is only possible to interact with the 'Connect' button and the text fields to fill in the patient data (Figures D.4). The initial state of the Interface is presented in the Figure D.1 in the Appendix.

The 'Connect' button allows to establish a connection between the Interface and the microcontroller via Serial Bluetooth. For the connection to be possible, the board must be paired with the Bluetooth of the laptop. Since it is being used Serial communication, it is necessary to select the COM port for the microcontroller and it should be the number 5 (it can be another port, but for this it is necessary to change the Python code for the corresponding port). A baud rate of 115200 must be defined for the COM port, as this was the value defined in the C++ code. If it is not possible to establish a connection, a warning message will appear (FigureD.2). If the connection is successful, the lamp turns green and other interface components become available to use, such as the 'Disconnect' button, the checkboxes for data selection and the 'Start Acquisition' button (Figure D.3), while the 'Connect' button becomes unavailable to use.

To start a acquisition, it is necessary to press the 'Start Acquisition' button. This button sends a message (the number 1) to the microcontroller to start the data collection. However, the message is only sent if at least one of the checkboxes corresponding to the data to be displayed in the graphics is selected. If none of the checkboxes is selected, a message appears with information to select the checkboxes corresponding to the data intended to be visualized (Figure D.5). In the checkboxes it is possible to select the muscle in which we want to see the activity (Pectoralis Major, Anterior Deltoid (AD), Medial Deltoid, Posterior Deltoid, Upper Trapezius and Lower Trapezius), as well as the kinematic data collected by the IMU (ACC and AV). The checkboxes can be seen in the Figure D.3.

Once the checkboxes are selected, the message can then be sent when the 'Start Acquisition' button is pressed, in order to start receiving data via Bluetooth. Because the EMG and IMU data are acquired at different rates, two different messages of different sizes are received, because the board reads the values from the six analog ports and there are also six kinematic parameters being acquired. One contains all the values associated with EMG activity and the number 1, while the other contains all the values corresponding to the kinematic parameters. The values received are distributed among the corresponding lists, for example, the second value of the EMG messages corresponds to the activity of the AD, which is assigned to a certain list, and each time a message with the EMG values is received, it is updated with the new value. In the end, the lists have different sizes and it is necessary to ensure that this is the same for all. To do this, the IMU data were assigned the value of 0 each time a message related to the EMG is received, and the same was applied to the EMG data when a message with IMU data is received. A list with the time variable in seconds was also created.

When an acquisition begins, the 'Stop Acquisition' button becomes available. When pressed, a message is sent to the microcontroller (the number 0) to stop the acquisition. After that, it is possible to interact with new buttons, such as, the 'Graphics', 'Save Data' and 'Save Plots'.

The 'Graphics' button opens a new window where all the plots can be visualized with their corresponding data, and each one has a color associated (Figure D.6). However, the signals will only appear in the plots that were previously selected in the checkboxes. The EMG plots

have their units in millivolts, the AV in radians per second and the ACC in g. It is important to mention that it was not possible to obtain plots with the data in real time because the laptop became too slow, which caused problems with the acquisition.

The 'Save Data' button allows the user to save the data collected by the microcontroller in a CSV file, which contains all the data read from the different ports, even those not selected in the checkboxes, since the microcontroller obtains and sends all the data from the different ports. The data is only possible to be saved, if all the patient's information has been filled in the text entries, because the name of the CSV file will contain all of this information. If the patient's data has not been filled in, a message will appear stating that this data is missing (Figure D.7).

The 'Save Plots' button saves a PNG file of the previously mentioned plots. Like the 'Save Data' button, the plots will only be saved if the patient information has been filled in.

To start a new acquisition, the 'Disconnect' button must be pressed first, because this button not only terminates the communication between the board and the laptop, and configures the interface back to its initial settings (the information in the checkboxes and in the text boxes doesn't disappear), but it also clears all the data from the lists.

4.4 Experimental protocol

The protocol used in this work for data acquisition is based on another that was developed and validated in another work, that is still under development. The original protocol includes ADL directed to the midline (drinking from a cup, eating soup and brushing teeth) and to the contralateral side (brushing the hair on the left side of the head and washing the left UL). The device used for data collections was the BiosignalsPlux (Plux Wireless Biosignals S.A., Portugal). The device has eight entries and six were used to acquire EMG data from six different muscles (Anterior, Medial and Posterior Deltoid, Upper and Lower Trapezius and Pectoralis Major) and the other two collected ACC in the X and Y axes using a accelerometer. The ACC in the Z-axis and AV were not recorded because there weren't enough entries in the device and it was not available a gyrcosope, respectively. Both EMG and ACC data were acquired at a sampling rate of 1000 Hz [14].

Due to available conditions and resources, the protocol had to undergo changes regarding the activities analyzed and data collected. During the work developed in this thesis only the activity of "Drinking from a cup"was studied. There was only one EMG sensor available, so just the AD muscle activity was collected. The skin was cleaned with alcohol and the electrodes were placed 2 cm apart on the same muscle, in the area of its belly, parallel to the muscle fibers, in order to obtain the best possible signal [71]. A reference electrode was placed on an area of low electrical activity, which in this case was the elbow. The placement of the electrodes is presented in the Figure 4.2. EMG data were acquired at a sampling rate of 1000 Hz. Since the IMU has an accelerometer and gyroscope, it was collected both raw ACC and raw AV, in the X, Y and Z axes. The sensor was placed on an armband around the arm near the elbow, with the Y-axis facing gravity, like it is presented in the Figure 4.3, with this orientation being chosen to

maintain coherence with the previous work [14]. The sensor was placed in this area since the goal is to study the arm movements adduction, abduction, rotations, extension and flexion, associated with the glenohuemral joint, that occur due to the activity of shoulder muscles [72]. The sampling rate chosen for the IMU data was 100 Hz because the studies mentioned in Chapter 3 that used IMU to record kinematic parameters applied a sampling rate ranging between 20 and 200 Hz [54], [56]–[58], [60].

Figure 4.2: Placement of electrodes on the Anterior Deltoid and elbow

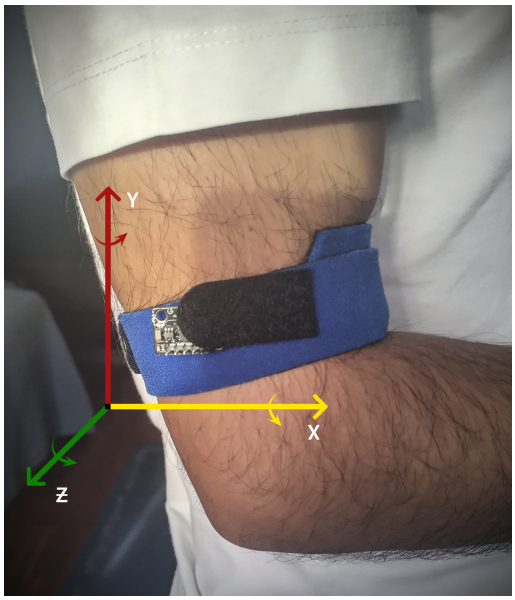

Figure 4.3: Orientation of the Inertial Measurement Unit when placed on the armband

The protocol was applied to healthy adult subjects, selected by convenience, who met the established sampling criteria.

Exclusion criteria were established: history of neuromotor or musculoskeletal pathology in the upper limbs, diagnosed cognitive or language deficits, changes in visual acuity not compensated by glasses or contact lenses [73], [74].

To carry out the study's experimental procedure, subjects had to read and sign a written informed consent before inclusion in the study, in accordance with the Declaration of Helsinki [75].

The task was performed five times with the dominant limb. Between these five cycles, the subjects had to completely rest their UL on the table and only then start the movement for the next cycle. This is an important part because it allows to distinguish the resting and moving moments in the EMG and IMU graphics [76]. Therefore, the task has this different moments:

1. Starting position until reaching the cup;
2. Grasping the cup;
3. Transporting the cup to the mouth;
4. Placing the cup in the mouth;
5. Returning the cup to pickup point;
6. Returning to starting position.

When an acquisition was made to a new subject, the board was reset. After each reset, the IMU values had to be adjusted. First, the IMU must be placed flat on a table, with the Z-axis in the direction of gravity, and it must be ensured that the ACC value in this axis is close to 1g and in the remaining axes close to 0g. If this does not happen, another reset must be made to the board, to ensure that the right values for ACC are being acquired. After confirming that the values are being read correctly, the IMU is then placed with the Y-axis in the direction of gravity to verify that the ACC value read in this axis is 1g. With this procedure done, the IMU could be placed in the armband and data collections could begin.

Before data collection itself, subjects had the opportunity to perform the activity movement once, so that they feel comfortable with performing the movement [76].

As soon as the subjects felt ready, an instruction to begin was given, after pressing the button to begin acquisition on the Interface, to carry out the activity at a speed that was comfortable for them.

For this task, a glass cup (10 cm high and 6 cm in diameter) was placed on a mark situated 30 cm from the edge of the table, facing to the midline [76].

The participants were seated in a chair without armrest (45 cm high), with the lumbar spine resting on the back of the chair, near a table (70 cm high, 80 cm wide and 65 cm deep), with the feet supported on the floor, knees and hip flexed at 90º. The ULs were placed on the table with the shoulder in neutral position, the elbow flexed at 90º, the forearm in pronation, the wrist in neutral position and the fingers in extension [76].

A phone was also included to record the activities in the frontal plane at a height of 90 cm and 100 cm towards the center of the table.

4.5 Data Processing

For signal processing, first, the signals collected from each participant (EMG activity in the AD, AV and ACC, the latter two containing the X, Y and Z axes) were processed individually. This aimed to visualize the signals of each participant to identify irregular patterns and exclude them from the final analysis of all the collected signals.

Each CSV file that was stored after each acquisition was uploaded to Matlab. As already mentioned, these files contain all the data collected by all ports of the microcontroller, regardless of whether or not the corresponding checkboxes were selected in the Interface.

Then, it was selected only the data of the signals that were intended to be analyzed, and the corresponding plots were visualized. An example of these signals for a given participant can be seen in the Figures E.1, E.2, E.3, E.4, E.5, E.6 and E.7 in the Appendix.

The '0' values assigned when the data were sent to their respective lists in Python were removed (Figures E.8, E.9, E.10, E.11, E.12, E.13 and E.14). This was done by selecting only the columns corresponding to EMG or IMU data, and if one of the instances had all of its values equal to 0, the respective row was eliminated.

A MAF was then applied to each signal to smooth it. The window used in MAFs refers to the number of data points included in the average at a given time. The average is computed by moving the window along the time series and recalculating the average for each window position. The value chosen for the window of the filter is the same as that applied in the sampling rates. However, when reviewing the data, it was found that the EMG sampling rate was too low, never exceeding 300 Hz. Therefore, the window size used for the EMG data was 300 (Figure E.15) and for the IMU data was 100 (Figures E.16, E.17, E.18, E.19, E.20 and E.21).

After obtaining the smoothed signals, only one of the five cycles was chosen to be analyzed, this being the fourth.

To define the limits of the fourth cycle and the phases of the movement, the videos were analyzed using the Adobe Premiere Pro software. The videos were cut by a few seconds at the beginning, in order to include only the moments in which data are actually being acquired. Then, the instants relating to the limits of the fourth cycle were identified. The time in the software appears in seconds and each video has a specific frames per second rate, which ranged from 29 to 41. To define the initial moment of the cycle, it was needed to choose the frame when the subjects started moving their UL, which was then converted to seconds. By dividing the frame chosen by the total number of frames per second of the video, and then add this value to the second in which the frame was, it is possible to know the instant when the cycle began.

For global processing, the first steps were similar to those described above. All of the participants data were uploaded into a single script, the '0s' were removed, the signal was truncated only have the fourth cycle, and the MAF was applied to that cycle only. The different signals

were then normalized, with the exception of the ACC data, because these values already vary between 0 and 1. For the EMG normalization, it was applied the formula presented in the Equation 4.5, and the values are comprehended between 0 and 1. The 'minVal' and 'maxVal' presented in this Equation, represent the minimum and maximum values of the smoothed signals. The AV normalization was done using the formula presented in Equation 4.6 and the values vary between -1 and 1. The 'maxabspos' represents the maximum of the absolute minimum and maximum values of the smoothed AV data. The data was resampled to ensure that the size was the same for all the plots of different subjects. For the EMG, a total of 2000 points was used for resampling and for the IMU, a total of 1000 points was used. In the Figures E.22, E.23, E.24 and E.25 it is presented the EMG activity and the AV of the UL normalized and resampled and in the Figures E.26, E.27 and E.28 it is presented the ACC resampled.

$$Normalized\ EMG\ Data = \frac{Resampled\ Data - minVal}{maxVal - minVal} \tag{4.5}$$

$$Normalized\ AV\ Data = \frac{Resampled\ Data}{maxabspos} \tag{4.6}$$

In the final plots, the mean and the Standard Deviation (SD) for the signals were presented. This plot also shows the mean instant and SD for each phase, which were determined using the videos and Excel. First, it was necessary to determine when the phases occurred for each participant using the videos, the same way as when the limits of the cycle were defined. Then, it was calculated the time between each phase for each participant, and the mean for these time differences was obtained. The values obtained were then added to each other, to obtain the mean moment for each phase and the mean duration of the cycles. These values were then converted from seconds to points, by applying the Equation 4.7 (the total number of points is different for the EMG and IMU data as mentioned previously). The SD was also calculated for each phase of the movement. This value was then converted to percentage using the Equation 4.8, and then converted to points through the Equation 4.9. These conversions to points are necessary due to data resampling, in order to present the mean instant and SD of the movement phases in the final plot.

$$Mean\ in\ Points = \frac{Mean\ Phase\ Time * Total\ Number\ of\ Points}{Mean\ Cycle\ Duration} \tag{4.7}$$

$$SD\ in\ \% = \frac{Phase\ SD * 100}{Mean\ Phase\ Time} \tag{4.8}$$

$$SD\ in\ Points = \frac{SD\ in\ \% * Total\ Number\ of\ Points}{100} \tag{4.9}$$

Chapter 5

Results and Data Analysis

This chapter presents the main results of this thesis. First, a brief description of the sample is given and then the results for the EMG and kinematic data are presented and discussed through a qualitative analysis. Furthermore, the EMG activity of the AD and ACC in the X and Y axes will also be compared with the data obtained by Garcia, to verify if there are resemblances between the results obtained by the prototype developed in this work with a commercially available device [14]. The ACC in the Z-axis and the AV in all three axes will not be compared, since these parameters were not obtained by Garcia [14].

5.1 Sample Characterization

The acquisitions were made in a group of 18 healthy people, of whom 11 (61.11%) were male and 7 (38.89%) female. Only one participant was left handed. 11 of them practice some kind of physical activity, but of these, only 3 practice a sport that involves a large ROM of the UL. Data about the sample characterization are presented in the Table 5.1.

Table 5.1: Sample Characterization

	Age	**Height (m)**	**Weight (kg)**
Interval	19-54	1,52-1,80	45-80
Mean	27	1.68	62.99
SD	10.29	0.087	7.58

5.2 Mean time and Standard Deviation values for the cycle and movement phases

The mean instant and SD for the movement phases corresponding to the EMG and kinematic data are presented in the Tables 5.2 and 5.3, respectively.

To obtain these values, only the data from the individuals used to obtain the final plots of the EMG signals and IMU parameters were taken into account. The reasons of why not all acquisitions were considered regarding a certain parameter will be explained later. Because of this, the mean instant for each phase and the SD value will vary depending on the parameter that is being analyzed.

Table 5.2: Mean instant and Standard Deviation values for the phases of the movement of the EMG data

	Phase 1	**Phase 2**	**Phase 3**	**Phase 4**	**Phase 5**	**Total**
Mean (s)	0,9543	1,1807	2,0897	3,4048	5,1065	6,6737
SD	0,1690	0,0861	0,3064	0,3818	0,3119	-

By analyzing the data in the Table 5.2, it is evident that participants required the most time to move the cup back to its initial position after it had been in their mouth. The shortest duration was between reaching and grasping the cup. The SD value is larger in phase four, corresponding to the moment when the person simulates that is drinking. Conversely, the SD is lower on phase two, which corresponds to grasping the cup.

Table 5.3: Mean instant and Standard Deviation values for the phases of the movement of the Inertial Measurement Unit data

	Phase 1	**Phase 2**	**Phase 3**	**Phase 4**	**Phase 5**	**Total**
Mean ACC (s)	1,0418	1,2879	2,2403	3,6527	5,5336	7,2059
Mean AV (s)	1,0421	1,2988	2,2477	3,6847	5,5817	7,2671
SD ACC	0,3006	0,13	0,3146	0,5737	0,519	-
SD AV	0,3192	0,1328	0,3285	0,6008	0,5501	-

The average duration of all phases increased for the IMU data, with the AV having a slight higher difference comparatively with the ACC. The SD also increased notably in phases four and five.

5.3 EMG

Only 14 of the 18 acquisitions were used in the EMG data analysis.

Some signals were affected by noise, and in order to try to reduce it, a MAF was directly applied in C++ code. Data were only collected on three subjects under these conditions and to maintain consistency with the previous work, the EMG data for these subjects were discarded.

Another individual's EMG data was rejected, because not only the fourth cycle but also the entire signal had an abnormal appearance compared to the rest. After analyzing the videos, it

was noticed that one of the electrodes was placed incorrectly in this subject, with this being placed between the AD and the Medial Deltoid, which ended up affecting the EMG signal acquired.

5.3.1 EMG Data Analysis and Data Comparison

In the Figure 5.1 it is possible to see the mean and the SD for the normalized EMG activity of the AD in the fourth cycle for all the individuals obtained in this work. The black lines indicate the average instant for the movement phases, while the colored lines demonstrate the respective SD.

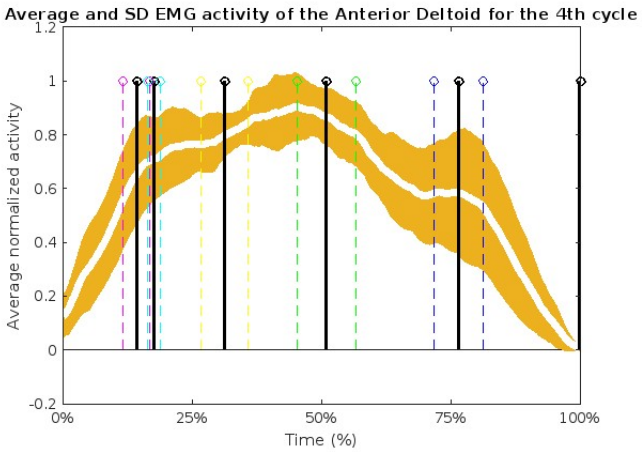

Figure 5.1: Mean and Standard Deviation for the normalized EMG activity of the Anterior Deltoid in the fourth cycle in all individuals, with the mean instant and Standard Deviation for the phases of the movement

By analyzing the graphic, it is apparent that three peaks are identifiable, which correspond to the most significant activation moments of the AD during the drinking task.

The first peak occurs when the subjects reached and grabbed the cup. To do this, the participants performed medial rotation and flexion of the shoulder, causing AD contraction.

The second is located near the middle of the cycle, during the instants when the subjects had the cup in contact with the mouth. In these moments, the subjects flexed and abducted the shoulder in order to take the cup to the mouth to simulate the act of drinking. It is also when the maximum moment of shoulder flexion occurs, with this being the reason of why this peak is the most prominent.

Once the subject returned the cup to its initial position, the AD started to relax, and the EMG activity declined, due to shoulder extension. Nevertheless, AD continued to contract, generating the third peak, when the participants returned the cup to its initial position.

The EMG activity then decreased, as the person returned to their initial position, and there was no more muscle contraction.

In the Figure 5.2, it is presented the activity of the AD obtained with the gold standard device [14]. Comparing this graphic with the one in the in Figure 5.1, it is possible to observe a

resemblance between the two. All three peaks occur around the same time and are associated with the respective phases of the movement.

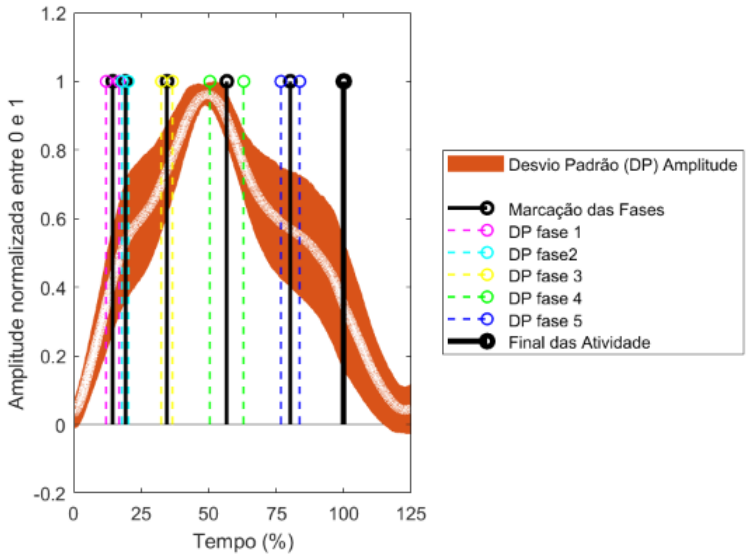

Figure 5.2: Mean and Standard Deviation for the normalized EMG activity of the Anterior Deltoid, with the mean instant and Standard Deviation for the phases of the movement obtained with the gold standard device [14]

However, the first peak in this study was more significant, and is almost at the same level as the second peak, which is the most noteworthy. This phenomenon can be attributed to the participants movement during the activity. In this study, some individuals began the movement with their UL not totally supported on the table, resting only their hand on it. This approach anticipates shoulder flexion when reaching the cup, in contrast with placing the forearms on the table, which mainly results in medial rotation. The activation of the AD is more significant during shoulder flexion as opposed to medial rotation.

It also affected the way the subjects returned to the original position. Instead of shoulder extension, the movement performed should have been external rotation. However, none of these movements causes contraction of the AD, so there are no major differences in the third peak.

Additionally, there is a difference in amplitude in the beginning and end of the movement. During the pause moments, there was a lot of noise in the signal, which affected its amplitude, by increasing it. In the previous work, there is also noise in these moments, but it is not as meaningful, with the EMG activity being lower and closer to 0 in these instants.

5.4 Angular Velocity

For the AV analysis, data from two participants were not included, due to drift in the signals leading consistently positive or negative AV values, which ended up affecting the mean and SD of the signals. The gyroscope tends to drift after short periods of time, in this case, after 5 to 10 minutes of being used, the sensor started to fail.

The AV signals from the left handed individual are reversed, as demonstrated in the Figures F.1, F.2, and F.3 in the Appendix. This was caused by the sensor's placement on the person's UL, that was identical to right handed people. In this case, as he was left handed, it ended up changing the direction of rotation of the axes. In order to include the data from this person, the AV values were inverted.

5.4.1 Angular Velocity Data Analysis

The Figures 5.3, 5.4 and 5.5, display the mean and SD for AV in the 3 axes, and the mean instant and SD for the phases of the movement.

AV measures the rate at which an object is changing its orientation while rotating around a central axis. If the AV is positive and it is increasing, it indicates an increase in the rotation speed in the counterclockwise direction. If the AV is positive and decreasing, there is a decrease in the rotation rate or the rotation stopped. If the AV shifts from positive to negative, the orientation of rotation changed. If the AV decreases even more, there is an increase in the rotation speed in the clockwise direction. When increases again, it suggests a slower rotation or there is no rotation at all. If the values return to positive, the direction of rotation changed once again.

Considering the sensor placement displayed in the Figure 4.3, it is possible to assume that adduction (rotations in the counterclockwise direction) and abduction (rotations in the clockwise direction) affect the X-axis (Figure 5.3), rotations (medial are associated with rotations in the counterclockwise orientation and external in the clockwise orientation) change the AV in the Y-axis (Figure 5.4) and flexion (rotations in the counterclockwise direction) and extension (rotations in the clockwise direction) the Z-axis (Figure 5.5).

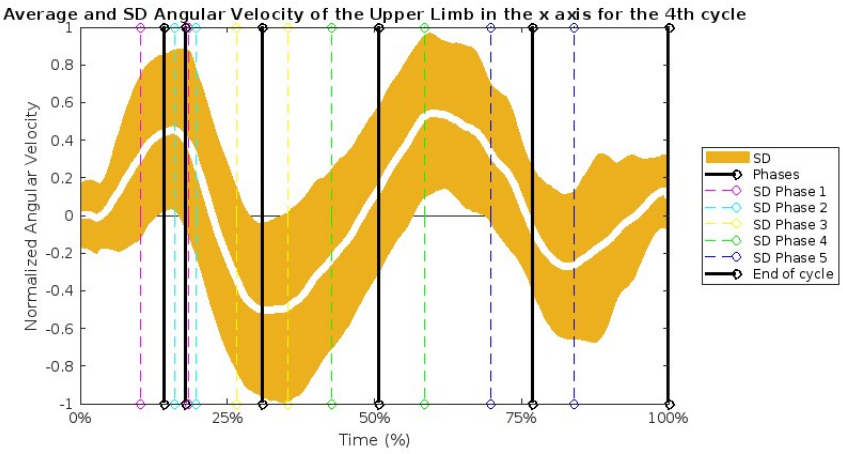

Figure 5.3: Mean and Standard Deviation for the normalized Angular Velocity in the X-axis the fourth cycle in all individuals, with the mean instant and Standard Deviation for the phases of the movement

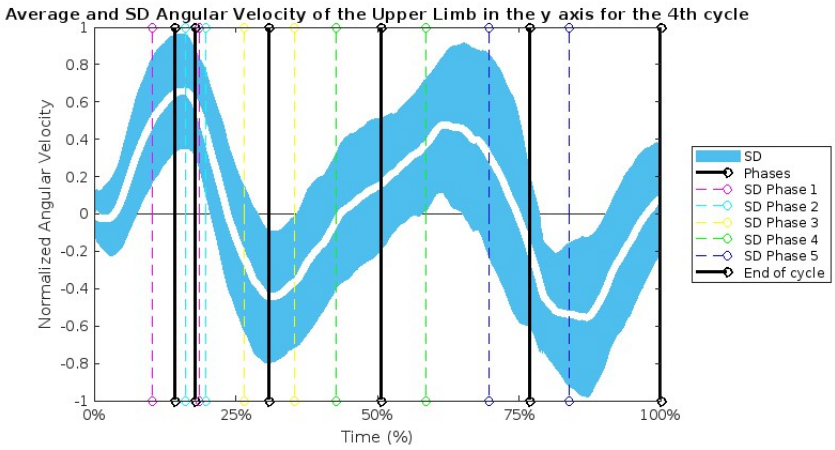

Figure 5.4: Mean and Standard Deviation for the normalized Angular Velocity in the Y-axis in the fourth cycle in all individuals, with the mean instant and Standard Deviation for the phases of the movement

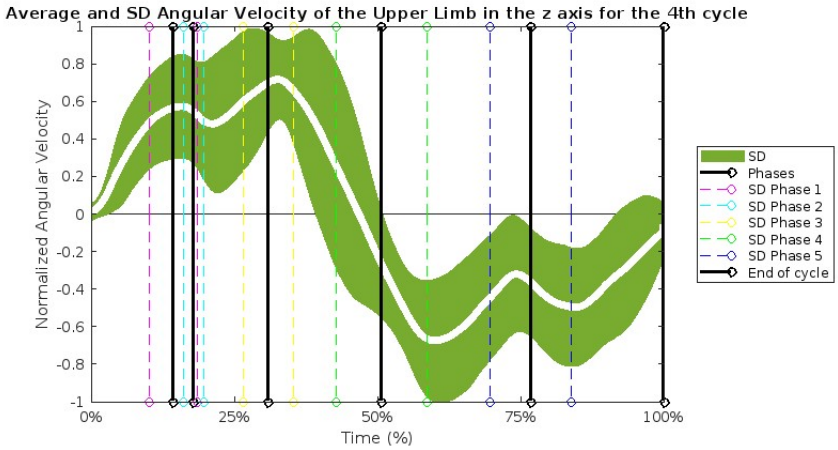

Figure 5.5: Mean and Standard Deviation for the normalized Angular Velocity in the Z-axis the fourth cycle in all individuals, with the mean instant and Standard Deviation for the phases of the movement

As mentioned in the EMG analysis, the movements performed by subjects to reach the cup in the first phase of the movement were medial rotation and shoulder flexion. In the AV plots, there is an increase in the Y and Z axes, which can be explained by these movements. Regarding the X-axis, initially there is a small decrease in the AV, followed by an increase. This can be explained, by existing a slight abduction when the hand leaves the table, followed by shoulder abduction when reaching the cup.

In the second phase of the movement, there is a slight decrease in the AV in all axes. These phases coincide with the moments when the subjects reached and grasped the cup, suggesting a reduction in angle variation due to minimal movement at the shoulder level.

In the third phase, there is a decrease X and Y AV and an increase in the Z-axis. As mentioned previously, when taking the cup to the mouth, the subjects must abduct and flex the shoulder, which affects the AV in the X and Z axes respectively. There is also external rotation of the shoulder, explained by the decrease in the Y-axis.

In the end of phase three, there is a negative AV peak in both X and Y, followed by an increase, which is caused by the lack of angle variation in phase four, with the values returning to 0. However, in the Z-axis, the peak occurs during phase four, indicating that there was still some shoulder flexion after the cup reached the mouth, followed by a decrease, suggesting that the movement was slowing down.

From approximately just before the end of phase four to roughly the midpoint of phase five, there is an increase in the AV of the axes X and Y and a decrease in the Z-axis. As already mentioned, when returning the cup to its initial position, the movements made were shoulder extension and adduction of the arm, which is verified by the behaviour of the Z and X axes, respectively. There was also medial rotation, verified by the increase in the Y-axis.

Just before the cup is left in its mark, the AV in all axes starts going to 0, due to the absence of movement. Upon release of the glass and subsequent return of the limb to its initial state, there is a decrease in the AV of all axes. This indicates that the movements necessary to return to the original position were abduction, external rotation, and shoulder extension. When the hand is back in its position, the values return to 0 due to less movement. However, there can still be some movements to adjust the position of the limb, mainly adduction and medial rotation, due to the increase that is verified in X and Y AV, respectively.

5.5 Acceleration

For the ACC analysis, all the signals collected from the subjects regarding this parameter were taken into account.

For the left handed person, the IMU placement only affected the ACC in the X-axis (Appendix F.4). As for AV, the signal was inverted to be used in the final graph.

5.5.1 Acceleration Data Analysis and Data Comparison

The Figures 5.6, 5.7, and 5.8 show the mean and SD for ACC in X, Y and Z axes, respectively, and the mean instant and SD for the phases of the movement.

The way to interpret ACC is different from AV. While AV was based on how a movement was being done around an axis, the ACC depends on the orientation of the axis in relation gravity. If an axis is facing gravity, its value will be about 1g (9.8 m/s^2), while the other axes should be closer to 0g.

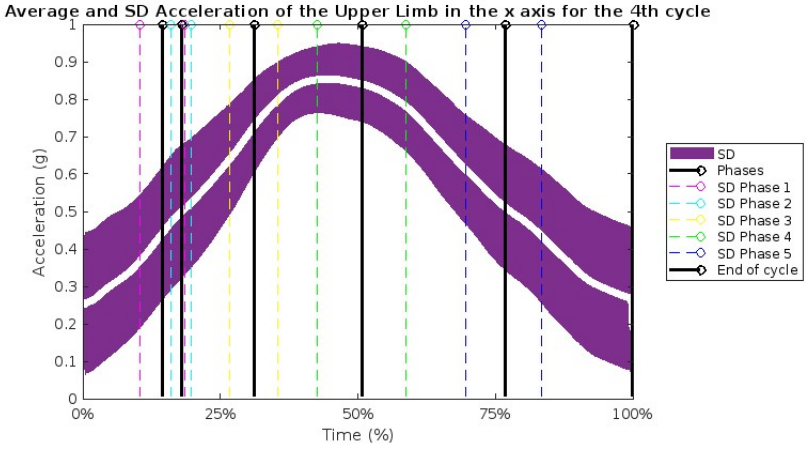

Figure 5.6: Mean and Standard Deviation for the Acceleration in the X-axis the fourth cycle in all individuals, with the mean and Standard Deviation in points for the phases of the movement

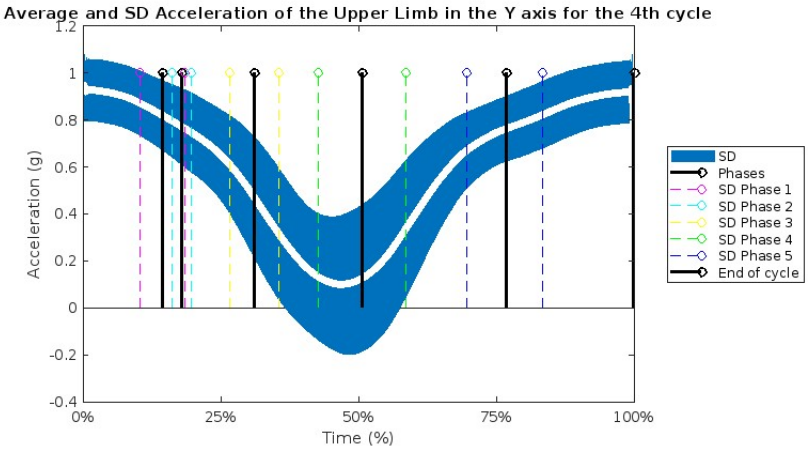

Figure 5.7: Mean and Standard Deviation for the Acceleration in the Y-axis the fourth cycle in all individuals, with the mean and Standard Deviation in points for the phases of the movement

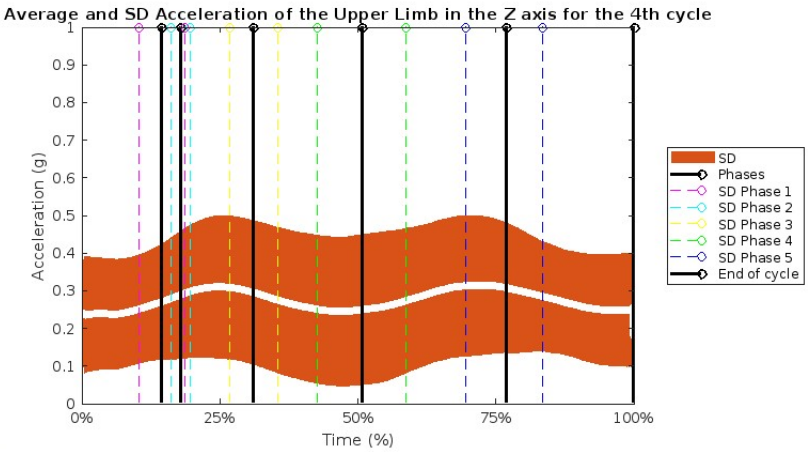

Figure 5.8: Mean and Standard Deviation for the Acceleration in the Z-axis the fourth cycle in all individuals, with the mean and Standard Deviation in points for the phases of the movement

Before the movement begins, the Y-axis is facing gravity and its value is near to 1g, while the ACC in other axes is near 0g. As the subjects reached the cup, the inclination started changing,

with the X-axis starting to face gravity and its value increasing, while the ACC in the Y-axis decreased. This change is primarily due to the shoulder flexion.

In phase three, the switch in ACC values between X and Y axes, becomes more notorious, due to shoulder flexion required for transporting the glass to the mouth. Once the cup reaches to the mouth, the shoulder continues to flex to simulate the act of drinking. This is when the ACC value in the X-axis reaches its maximum value of nearly 1g, as this axis is facing gravity, while the ACC in the Y-axis reaches its lowest value, almost at 0g.

When the cup leaves the mouth and returns to the initial position, the movement that allows this transportation, is shoulder extension. This causes the sensor inclination to change once again, hence resetting the ACC values in both X and Y to their initial state.

The Z-axis ACC doesn't have much variation as most of the movement occurs in the sagittal plane. This is because shoulder flexion and extension are the main actions responsible for bringing the cup to the mouth. In order to have more variation of ACC value in the Z-axis, abduction or adduction movements need to occur to make the axis face gravity. Based on the graphic, it can be inferred that rising ACC levels coincide with abduction motions, such as when the person lifts the cup to the mouth and when places it back on the table, while decreases align with adduction, such as when the subject simulates that is drinking and when returns the limb to the initial position.

The ACC in the X and Z axes is a bit higher than expected, especially at the beginning and end of the movement. This may be explained due to signal noise, which affected the average ACC in these axes. Ideally, the ACC should be close to 0g in these axes at the start and end, as the Y-axis is the axis that faces gravity.

In the Figure 5.9, it is represented the ACC value in the X-axis obtained with the gold standard device [14]. Comparing this graphic with the one in the Figure 5.6, there are some resemblances. The ACC value for the X-axis in this study demonstrates a greater increase during the first three phases of the movement, in contrast with the results presented in the Figure 5.9 where values remain mostly constant in the first two phases and only increase when the cup is lifted towards the mouth. Both acceleration values almost reach 1g. However, in the prior research study, this reading was recorded when at the end of phase four, while in this study, the peak value is identified between phases three and four. During the final phase of the movement, both ACCs decrease, but in the Figure 5.9, the ACC is more stable in this stage. The discrepancies observed in the initial and final phases of the movement, can be attributed to the positioning of the limb on the table.

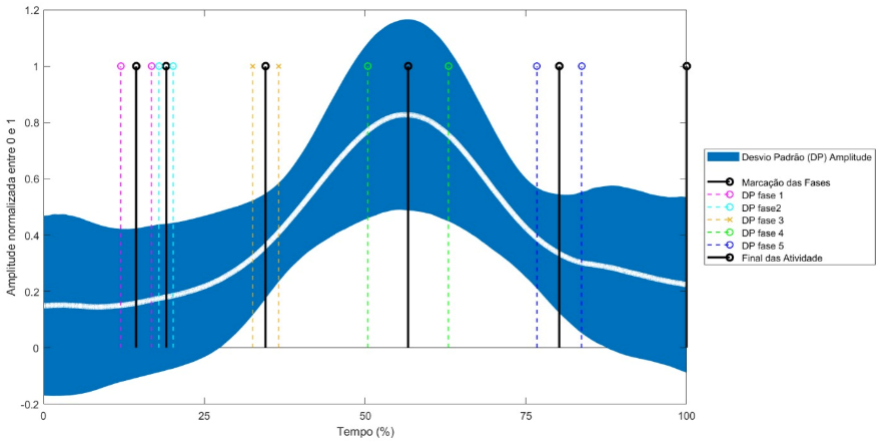

Figure 5.9: Mean and Standard Deviation for the Acceleration in the X-axis, with the mean and Standard Deviation in points for the phases of the movement obtained by Garcia [14]

In the Figure 5.10, it is represented the ACC in the Y-axis obtained with the gold standard device [14]. The shape of the signal is similar to the one obtained in this work, but there are some differences. In the previous work, there is a fluctuation in the first three phases of the movement, with the value only decreasing moments before the cup arrives at the mouth. In this work, the ACC value in the Y-axis starts decreasing right from the beginning of the movement. Both signals reach nearly 0g, but the minimum peak occurs precisely when the cup departs from the mouth, whereas in this study, the peak arises a few moments before the end of phase four. Upon placing the glass back in its original position, there is an increase followed by a decrease as presented in the Figure 5.10, whereas in the current study the ACC only increases until the end of the movement. The dissimilarity between the plots in the initial and final moments of the cycle can also be attributed to the starting position of the limb on the table.

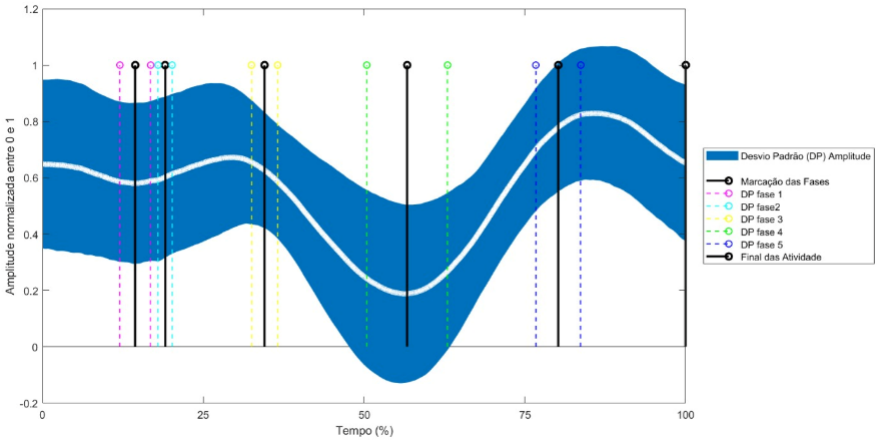

Figure 5.10: Mean and Standard Deviation for the Acceleration in the Y-axis, with the mean and Standard Deviation in points for the phases of the movement obtained by Garcia [14]

As previously discussed, placing only the hand on the table results in shoulder flexion when reaching for the cup. This approach causes an earlier change in the sensor's inclination. Alternatively, placing the forearm on the table brings the limb closer to the cup, and the primary

movement to reach it is medial rotation, which has little effect on the sensor's orientation towards gravity, with the Y-axis facing gravity during this moments. When returning the limb to the initial position, the movement that should have been done was external rotation, instead of shoulder extension, which would also have less effect in the sensor's inclination. These are the reasons why the values obtained by Garcia regarding the acceleration in the X and Y axes are more stable during the initial and final phases of the movement, since the inclination of the sensor almost does not change in these instants.

The difference in the sampling rates can also affect the results obtained, since the acquisitions made with the gold standard device have a higher acquisition rate. The number of points collected is substantially lower, due to the use of 100 Hz instead of 1000 Hz, with less information about the kinematic parameters of the movement being acquired.

5.6 Limitation of the study

This work has several limitations that affected the final results.

The literature suggests that the sampling sate for EMG data should be at least 1000 Hz, and was the value used in the previous work [31]. However, as mentioned in Section 4.5, the sampling rate never exceeded 300 Hz. This is problematic because EMG requires higher acquisition rates in order to obtain the maximum possible information about the signal. The C++ code must be reviewed to attempt an increase in this value. There can be some flaws in the Serial Bluetooth data transmission, which reduced the sampling rate. The code may also not be able to process all the information due to limitations in processing power of the microcontroller or communication bandwidth. The use of print statements to send the data may also influence the sampling rate, because the microcontroller must divert some of its processing power to handle these operations.

The analysis only focused on one muscle and one ADL, whereas the previous study examined the activity of six muscles during various ADL. This was due to time constraints and also lack of sensors to study more muscles. By assessing muscular activity across different muscles, it becomes possible to comprehend how the distinct muscles of the shoulders collaborate to produce a given movement. With more activities performed, it would be also possible to compare the activity of the different muscles in a set of different ADL.

The BiosignalsPlux was not used for any data collection in this study. While the results for AD activity and ACC in the Y and X axes during the drinking task align with the previous study, data should have been collected using both devices simultaneously, to ensure a more accurate validation of the developed device. Every people executes the movement differently, and by using both devices, it is possible to see if there are any major differences in the signals obtained from each person.

The conditions under which the tests were conducted were different than those in the prior work. The table and chair utilized were distinct, with the table being substantially taller. Due to this, the initial limb position changed to ensure a 90º angle at the elbow joint. The majority of participants supported only their hands on the table, which forces shoulder flexion to be

the primary movement at the beginning of the activity and shoulder extension in the end of it. This explains the prominence of the first peak in the EMG signal compared to the previous work, the subsequent increase in AV in the Z-axis in the first phase of the movement and the decrease of the AV also in this axis in the end of the movement, and the differences verified in the ACC in the X and Y axes comparatively to the results obtained with the gold standard device. The forearm should have been fully supported on the table for improved coherence with the acquisitions made in the work. In this position, the initial movement performed would be primarily medial rotation, resulting in lower activation of the AD, a lower AV in the X and Z axes, while the Y-axis would have a bigger increase, and the ACC plots in the X and Y axes would be more similarly to the ones obtained with the gold standard device. When returning the limb to the initial position, the movement performed would be external rotation instead of shoulder extension, and changes would also be visible in the AV in the Y and Z axes and in the ACC in the X and Y axes. Additionally, another movement was observed in shorter individuals, who had more difficulty reaching the glass, which was shoulder abduction.

Random movements made by participants, such as adjusting their position on the chair, affected the signals, specially in the resting moments.

The majority of the EMG signals were affected by noise, which created a problem, particularly during the resting moments, when the UL remains stationary between cycles. During these instances, the EMG activity should have been closer to 0, but in some signals the values were quite high. As a result, it adversely impacted both the start and end of the cycles. The sources of the interference may stem from either an improper placement of the electrodes, specially the reference electrode, or the microcontroller's power supply. When the board was directly connected to the power supply or to the laptop while charging, were the moments where some noise was visible. Further testes must be done, in order to verify the origins of the noise.

Regarding the IMU sensor, the accelerometer (ACC) was also subject to noise, although it is considered normal for this type of sensor, and the gyroscope suffered from drift when used for longs periods of time. More resets should have been done to the board, in order to recalibrate the IMU sensor to get more accurate results.

Additionally, there were issues with the videos that were recorded using a telephone, each with a different frame rate ranging from 29 to 41 fps. When selecting the limits of the cycle and the movement phases, the chosen moment may not be entirely accurate. To solve this, a camera with a fixed frame per second rate should be used.

CHAPTER 6

CONCLUSION AND FUTURE PERSPECTIVES

In order to achieve the main goals, it was necessary to program a microcontroller. A code previously written in C++ specifically designed to obtain IMU orientation through Madgwick filter was used. The code was modified to allow the acquisition of all desired parameters and to work via Bluetooth. A interface was developed in Python for communicating with the device. Through this, the user can establish a connection with the microcontroller, select the desired data to be seen, fill in personal information about the patient, send commands to start transmitting data via Bluetooth and stop the acquisition, see the data in the specified plots, save the data into a CSV file in the laptop and save a PNG file with the data displayed in the graphics.

To determine if the device was capable of collecting data correctly, acquisitions were made in a sample of healthy people. EMG data was collected from the Anterior Deltoid, and the raw acceleration and angular velocity from an IMU, while studying the Activity of Daily Living of drinking water from a cup. Results were compared with acquisitions made with a device already commercially available and validated. This is an important research objective, as there is a lack of studies that analyze both EMG and kinematic parameters during ADL. The initial data collection from healthy individuals can establish a normative pattern of upper limb function under typical conditions and subsequently inform the evaluation of individuals with neurological conditions. This ultimately facilitates the identification of functional impairments and the development of tailored rehabilitation plans.

The obtained results are promising because they exhibit similarity in acquired parameters from both studies. The EMG plots have identical formats, showing three discernible activity peaks. However, this study's first EMG peak amplitude is comparatively higher than the one obtained due to the type of movement performed. The acceleration behavior in the Y and X axes is consistent in both studies, but there are some differences at the initial and final moments of the movement, due to the positioning of limb in these periods.

Overall the objectives of this project were achieved. However, it should be noted that the device is currently only in prototype stage and the tests conducted were focused solely on its ability to collect data and verify the functionality of the Interface. Further improvements and studies are required before its use in clinical facilities can be considered.

The microcontroller was powered directly through electrical current during this project. This may potentially introduce noise into the EMG signals. Additionally, since wireless functionality is a requirement, an alternative power source such as a power bank or battery must be employed.

Furthermore, addressing the issues with the EMG sampling rate, which is currently too low, is crucial to ensure proper EMG acquisition. Instead of multiple prints with the different data being acquired, variables gathering all the information about the data can be created, in order to try to reduce the processing power.

To validate the device accurately, it is recommended to conduct acquisitions using both the device developed in this study and BiosignalsPlux at the same time, while collecting data in one individual. Additionally, studying the EMG activity in multiple muscles and during various activities in healthy individuals would not only aid in the device validation process but also facilitate an investigation of the Upper Limb behavior during different Activities of Daily Living. If positive results are obtained, further studies should consider analyzing these parameters in stroke patients as the goal is to implement this product in clinical settings.

It is also necessary to test and validate the orientation of the IMU obtained with the Madgwick filter using OS resources. Upgrading the IMU to a MARG sensor can provide more accurate orientation information, but this would require a different code for the sensor to work.

The placement of the IMU in left handed people should be reconsidered, in order to obtain the signals from angular velocity and acceleration in the X axis more similar to right handed people. To solve this, the IMU sensor must be placed in the interior part of the arm. This way, the axes and the rotation sense would be aligned in the same way regardless of the dominant limb.

Bibliography

[1] J. M. Lourenço, *The NOVAthesis LaTeX Template User's Manual*, NOVA University Lisbon, 2021. [Online]. Available: https://github.com/joaomlourenco/novathesis/raw/master/template.pdf.

[2] D. J. Magermans, E. K. Chadwick, H. E. Veeger, and F. C. V. D. Helm, "Requirements for upper extremity motions during activities of daily living", *Clinical biomechanics (Bristol, Avon)*, vol. 20, pp. 591–599, 6 2005-07. DOI: 10.1016/J.CLINBIOMECH.2005.02.006.

[3] J. Eraifej, W. Clark, B. France, S. Desando, and D. Moore, "Effectiveness of upper limb functional electrical stimulation after stroke for the improvement of activities of daily living and motor function: A systematic review and meta-analysis", *Systematic Reviews*, vol. 6, 1 2017-02. DOI: 10.1186/S13643-017-0435-5.

[4] M. Coscia, M. J. Wessel, U. Chaudary, *et al.*, "Neurotechnology-aided interventions for upper limb motor rehabilitation in severe chronic stroke", *Brain*, vol. 142, p. 2182, 8 2019-08. DOI: 10.1093/BRAIN/AWZ181.

[5] C. Angerhöfer, A. Colucci, M. Vermehren, V. Hömberg, and S. R. Soekadar, "Post-stroke rehabilitation of severe upper limb paresis in germany – toward long-term treatment with brain-computer interfaces", *Frontiers in Neurology*, vol. 12, p. 772 199, 2021-11. DOI: 10.3389/FNEUR.2021.772199.

[6] M. F. Levin, J. A. Kleim, and S. L. Wolf, "What do motor "recovery"and "compensation"mean in patients following stroke?", *Neurorehabilitation and neural repair*, vol. 23, pp. 313–319, 4 2009-05. DOI: 10.1177/1545968308328727.

[7] A. M. Oosterwijk, M. K. Nieuwenhuis, C. P. van der Schans, and L. J. Mouton, "Shoulder and elbow range of motion for the performance of activities of daily living:a systematic review", *Physiotherapy Theory and Practice*, vol. 34, pp. 505–528, 7 2018-07. DOI: 10.1080/09593985.2017.1422206.

[8] "Guidelines for adult stroke rehabilitation and recovery: A guideline for healthcare professionals from the american heart association/american stroke association", *Stroke*, vol. 47, e98–e169, 6 2016-06. DOI: 10.1161/STR.0000000000000098.

[9] N. Hussain, K. S. Sunnerhagen, and M. A. Murphy, "End-point kinematics using virtual reality explaining upper limb impairment and activity capacity in stroke", *Journal of NeuroEngineering and Rehabilitation*, vol. 16, 1 2019-07. DOI: 10.1186/S12984-019-0551-7.

[10] I. A. Mesquita, P. F. P. da Fonseca, A. R. V. Pinheiro, M. F. P. V. Correia, and C. I. C. da Silva, "Methodological considerations for kinematic analysis of upper limbs in healthy and poststroke adults part ii: A systematic review of motion capture systems and kinematic metrics", *Topics in Stroke Rehabilitation*, vol. 26, pp. 464–472, 6 2019-08. DOI: 10.1080/10749357.2019.1611221.

[11] F. Coupar, A. Pollock, P. Rowe, C. Weir, and P. Langhorne, "Predictors of upper limb recovery after stroke: A systematic review and meta-analysis", *Clinical Rehabilitation*, vol. 26, pp. 291–313, 4 2012-04. DOI: 10.1177/0269215511420305.

[12] D. H. Gates, L. S. Walters, J. Cowley, J. M. Wilken, and L. Resnik, "Range of motion requirements for upper-limb activities of daily living", *The American Journal of Occupational Therapy*, vol. 70, 70013500 10p1, 1 2016-01. DOI: 10.5014/AJOT.2016.015487.

[13] A. Schwarz, C. M. Kanzler, O. Lambercy, A. R. Luft, and J. M. Veerbeek, "Systematic review on kinematic assessments of upper limb movements after stroke", *Stroke*, vol. 50, pp. 718–727, 3 2019-03. DOI: 10.1161/STROKEAHA.118.023531.

[14] I. I. C. Garcia, *Estudo integrado de análise biomecânica do membro superior e eletromiografia em indivíduos sem patologia associada*, 2023 (In progress).

[15] P. Santos, C. Quaresma, I. Garcia, and C. Quintão, *Neuromotor evaluation of the upper limb during activities of daily living: A pilot study*.

[16] M. P. A. Gómez, F. Aparisi, G. Battista, G. Guglielmi, C. Faldini, and A. Bazzocchi, "Functional and surgical anatomy of the upper limb: What the radiologist needs to know", *Radiologic clinics of North America*, vol. 57, pp. 857–881, 5 2019-09. DOI: 10.1016/J.RCL.2019.03.002.

[17] W. Bakhsh and G. Nicandri, "Anatomy and physical examination of the shoulder", *Sports Medicine and Arthroscopy Review*, vol. 26, e10–e22, 3 2018-09. DOI: 10.1097/JSA.0000000000000202.

[18] E. Pina, *Anatomia da Locomoção*, 5th ed. Lidel, 2017.

[19] J. Tu, K. Inthavong, and G. Ahmadi, "Reconstruction of the human airways", in 1st ed. Springer, Dordrecht, 2013, pp. 45–71. DOI: 10.1007/978-94-007-4488-2_3.

[20] R. Kadi, A. Milants, and M. Shahabpour, "Shoulder anatomy and normal variants", *Journal of the Belgian Society of Radiology*, vol. 101, Suppl 2 2017. DOI: 10.5334/JBR-BTR.1467.

[21] S. Health. "Guide to shoulder anatomy | sports-health". (), [Online]. Available: https://www.sports-health.com/sports-injuries/shoulder-injuries/guide-shoulder-anatomy. Accessed on: 26, February 2023.

[22] M. Wong and J. Kiel, "Anatomy, shoulder and upper limb, acromioclavicular joint", in StatPearls Publishing, 2022-07.

[23] L.-R. Chang, P. Anand, and M. Varacallo, "Anatomy, shoulder and upper limb, glenohumeral joint", in StatPearls Publishing, 2022-08.

[24] T. N. Epperson and M. Varacallo, "Anatomy, shoulder and upper limb, sternoclavicular joint", in StatPearls Publishing, 2022-07.

[25] S. P. Explained. "Muscles of the shoulder: Anatomy, function common injuries". (), [Online]. Available: https://www.shoulder-pain-explained.com/muscles-of-the-shoulder.html. Accessed on: February, 21, 2023.

[26] C. McCausland, E. Sawyer, B. J. Eovaldi, and M. Varacallo, "Anatomy, shoulder and upper limb, shoulder muscles", in StatPearls Publishing, 2022-08.

[27] M. P. Clinic. "Shoulder muscles anatomy, exercise, name list : -". (), [Online]. Available: https://mobilephysiotherapyclinic.in/shoulder-muscles-anatomy-exercise-name-list/. Accesed on: February, 21, 2023.

[28] M. del Olmo and R. Domingo, "Emg characterization and processing in production engineering", *Materials*, vol. 13, pp. 1–28, 24 2020-12. DOI: 10.3390/MA13245815.

[29] W. R. Frontera and J. Ochala, "Skeletal muscle: A brief review of structure and function", *Behavior Genetics*, vol. 45, pp. 183–195, 2 2015-03. DOI: 10.1007/S00223-014-9915-Y.

[30] M. Raghavan, D. Fee, and P. E. Barkhaus, "Generation and propagation of the action potential", *Handbook of Clinical Neurology*, vol. 160, pp. 3–22, 2019-01. DOI: 10.1016/B978-0-444-64032-1.00001-1.

[31] P. Konrad, *The ABC of EMG*, 1st ed. Noraxon, 2006.

[32] B. McHugh, B. Akhbari, A. M. Morton, D. C. Moore, and J. J. Crisco, "Optical motion capture accuracy is task-dependent in assessing wrist motion", *Journal of biomechanics*, vol. 120, p. 110 362, 2021-05. DOI: 10.1016/J.JBIOMECH.2021.110362.

[33] U. G. Longo, S. D. Salvatore, A. Carnevale, *et al.*, "Optical motion capture systems for 3d kinematic analysis in patients with shoulder disorders", *International journal of environmental research and public health*, vol. 19, 19 2022-10. DOI: 10.3390/IJERPH191912033.

[34] M. Al-Amri, K. Nicholas, K. Button, V. Sparkes, L. Sheeran, and J. L. Davies, "Inertial measurement units for clinical movement analysis: Reliability and concurrent validity", *Sensors 2018, Vol. 18, Page 719*, vol. 18, p. 719, 3 2018-02. DOI: 10.3390/S18030719.

[35] OptiTrack. "Optitrack - motion capture systems". (), [Online]. Available: https://optitrack.com/. Accessed on: September, 18, 2023.

[36] S. B. Farahan, J. J. Machado, F. G. de Almeida, and J. M. R. Tavares, "9-dof imu-based attitude and heading estimation using an extended kalman filter with bias consideration", *Sensors (Basel, Switzerland)*, vol. 22, 9 2022-05. DOI: 10.3390/S22093416.

[37] B. Guignard, O. Ayad, H. Baillet, *et al.*, "Validity, reliability and accuracy of inertial measurement units (imus) to measure angles: Application in swimming", *Sports Biomechanics*, 2021. DOI: 10.1080/14763141.2021.1945136.

[38] M. P. van Dijk, M. Kok, M. A. Berger, M. J. Hoozemans, and D. J. H. Veeger, "Machine learning to improve orientation estimation in sports situations challenging for inertial sensor use", *Frontiers in sports and active living*, vol. 3, 2021-08. DOI: 10.3389/FSPOR.2021.670263.

[39] S. O. Madgwick, A. J. Harrison, and R. Vaidyanathan, "Estimation of imu and marg orientation using a gradient descent algorithm", *IEEE ... International Conference on Rehabilitation Robotics : [proceedings]*, vol. 2011, 2011. DOI: 10.1109/ICORR.2011.5975346.

[40] M. A. Wirth, G. Fischer, J. Verdú, L. Reissner, S. Balocco, and M. Calcagni, "Comparison of a new inertial sensor based system with an optoelectronic motion capture system for motion analysis of healthy human wrist joints", *Sensors (Basel, Switzerland)*, vol. 19, 23 2019-12. DOI: 10.3390/S19235297.

[41] M. L. Hoang and A. Pietrosanto, "Yaw/heading optimization by machine learning model based on mems magnetometer under harsh conditions", *Measurement*, vol. 193, p. 111 013, 2022-04. DOI: 10.1016/J.MEASUREMENT.2022.111013.

[42] Y. Zhou, H. Cao, and T. Guo, "A hybrid algorithm for noise suppression of mems accelerometer based on the improved vmd and tfpf", *Micromachines*, vol. 13, 6 2022-06. DOI: 10.3390/MI13060891.

[43] A. Iluk, "Flight controller as a low-cost imu sensor for human motion measurement", *Sensors*, vol. 23, 4 2023-02. DOI: 10.3390/S23042342/S1.

[44] J. P. Branco, S. Oliveira, J. P. Pinheiro, and P. L. Ferreira, "Assessing upper limb function: Transcultural adaptation and validation of the portuguese version of the stroke upper limb capacity scale", *BMC Sports Science, Medicine and Rehabilitation*, vol. 9, 1 2017-08. DOI: 10.1186/S13102-017-0078-9.

[45] WHO. "International classification of functioning, disability and health (icf)". (), [Online]. Available: https://www.who.int/standards/classifications/international-classification-of-functioning-disability-and-health. Accessed on: February, 14, 2023.

[46] M. McDonnell, "Action research arm test: Commentary", *Australian Journal of Physiotherapy*, vol. 54, p. 220, 3 2008. DOI: 10.1016/S0004-9514(08)70034-5.

[47] D. J. Gladstone, C. J. Danells, and S. E. Black, "The fugl-meyer assessment of motor recovery after stroke: A critical review of its measurement properties", *Neurorehabilitation and Neural Repair*, vol. 16, pp. 232–240, 3 2002. DOI: 10.1177/154596802401105171.

[48] R. D. Barbell. "Types of gpp: Bilateral vs unilateral vs ipsilateral vs contralateral – red dragon barbell". (), [Online]. Available: https://reddragonbarbell.wordpress.com/2021/05/03/types-of-gpp-bilateral-vs-unilateral-vs-ipsilateral-vs-contralateral/. Accessed on: December, 18, 2023.

[49] K. Kim, W. K. Song, J. Lee, *et al.*, "Kinematic analysis of upper extremity movement during drinking in hemiplegic subjects", *Clinical biomechanics (Bristol, Avon)*, vol. 29, pp. 248–256, 3 2014. DOI: 10.1016/J.CLINBIOMECH.2013.12.013.

[50] T. McGrath and L. Stirling, "Body-worn imu-based human hip and knee kinematics estimation during treadmill walking", *Sensors (Basel, Switzerland)*, vol. 22, 7 2022-04. DOI: 10.3390/S22072544.

[51] E. P. Washabaugh, T. Kalyanaraman, P. G. Adamczyk, E. S. Claflin, and C. Krishnan, "Validity and repeatability of inertial measurement units for measuring gait parameters", *Gait posture*, vol. 55, pp. 87–93, 2017-06. DOI: 10.1016/J.GAITPOST.2017.04.013.

[52] N. Reneaud, R. Zory, O. Guérin, *et al.*, "Validation of 3d knee kinematics during gait on treadmill with an instrumented knee brace", *Sensors (Basel, Switzerland)*, vol. 23, 4 2023-02. DOI: 10.3390/S23041812.

[53] T. Provot, X. Chiementin, E. Oudin, F. Bolaers, and S. Murer, "Validation of a high sampling rate inertial measurement unit for acceleration during running", *Sensors (Basel, Switzerland)*, vol. 17, 9 2017-09. DOI: 10.3390/S17091958.

[54] J. Henschke, H. Kaplick, M. Wochatz, and T. Engel, "Assessing the validity of inertial measurement units for shoulder kinematics using a commercial sensor-software system: A validation study", *Health Science Reports*, vol. 5, 5 2022-09. DOI: 10.1002/HSR2.772.

[55] M. Rigoni, S. Gill, S. Babazadeh, *et al.*, "Assessment of shoulder range of motion using a wireless inertial motion capture device—a validation study", *Sensors (Basel, Switzerland)*, vol. 19, 8 2019-04. DOI: 10.3390/S19081781.

[56] M. M. Morrow, B. Lowndes, E. Fortune, K. R. Kaufman, and M. S. Hallbeck, "Validation of inertial measurement units for upper body kinematics", *Journal of applied biomechanics*, vol. 33, p. 227, 3 2017-06. DOI: 10.1123/JAB.2016-0120.

[57] L. Y. T. Chan, C. S. Chua, S. M. Chou, *et al.*, "Assessment of shoulder range of motion using a commercially available wearable sensor-a validation study", *mHealth*, vol. 8, pp. 30–30, 2022-10. DOI: 10.21037/MHEALTH-22-7.

[58] H. S. Nam, W. H. Lee, H. G. Seo, M. W. Smuck, and S. Kim, "Evaluation of motion segment size as a new sensor-based functional outcome measure in stroke rehabilitation", *The Journal of International Medical Research*, vol. 50, pp. 1–10, 9 2022-09. DOI: 10.1177/03000605221122750.

[59] B. Kirking, M. El-Gohary, and Y. Kwon, "The feasibility of shoulder motion tracking during activities of daily living using inertial measurement units", *Gait and Posture*, vol. 49, pp. 47–53, 2016-09. DOI: 10.1016/J.GAITPOST.2016.06.008.

[60] J. P. Held, B. Klaassen, A. Eenhoorn, *et al.*, "Inertial sensor measurements of upper-limb kinematics in stroke patients in clinic and home environment", *Frontiers in Bioengineering and Biotechnology*, vol. 6, p. 12, APR 2018-04. DOI: 10.3389/FBIOE.2018.00027/FULL.

[61] S. W. Alpert, M. M. Pink, F. W. Jobe, P. J. McMahon, and W. Mathiyakom, "Electromyographic analysis of deltoid and rotator cuff function under varying loads and speeds", *Journal of Shoulder and Elbow Surgery*, vol. 9, pp. 47–58, 1 2000. DOI: 10.1016/S1058-2746(00)90009-0.

[62] T. J. Brindle, A. J. Nitz, T. L. Uhl, E. Kifer, and R. Shapiro, "Kinematic and emg characteristics of simple shoulder movements with proprioception and visual feedback", *Journal of Electromyography and Kinesiology*, vol. 16, pp. 236–249, 3 2006-06. DOI: 10.1016/J.JELEKIN.2005.06.012.

[63] D. A. Gabriel, "Shoulder and elbow muscle activity in goal-directed arm movements", *Experimental brain research*, vol. 116, pp. 359–366, 2 1997. DOI: 10.1007/PL00005763.

[64] O. Levin, A. Forner-Cordero, Y. Li, M. Ouamer, and S. Swinnen, "Evidence for adaptive shoulder-elbow control in cyclical movements with different amplitudes, frequencies, and orientations", *Journal of Motor Behaviour*, vol. 40, pp. 499–515, 6 2010-11. DOI: 10.3200/JMBR.40.6.499-515.

[65] F. P. F. Ricci, P. R. P. Santiago, A. C. Zampar, L. N. Pinola, and M. de Cássia Registro Fonseca, "Upper extremity coordination strategies depending on task demand during a basic daily activity", *Gait posture*, vol. 42, pp. 472–478, 4 2015-10. DOI: 10.1016/J.GAITPOST.2015.07.061.

[66] E. Repnik, U. Puh, N. Goljar, M. Munih, and M. Mihelj, "Using inertial measurement units and electromyography to quantify movement during action research arm test execution", *Sensors (Basel, Switzerland)*, vol. 18, 9 2018-09. DOI: 10.3390/S18092767.

[67] WallySci. "Home | wallysci". (), [Online]. Available: https://www.wallysci.com/. Accessed on: February, 22, 2023.

[68] S. Y. Shin, Y. Kim, A. Jayaraman, and H. S. Park, "Relationship between gait quality measures and modular neuromuscular control parameters in chronic post-stroke individuals", *Journal of NeuroEngineering and Rehabilitation*, vol. 18, pp. 1–12, 1 2021-12. DOI: 10.1186/S12984-021-00860-0/TABLES/3.

[69] K. Winer. "Github - kriswiner/mpu6050: Basic mpu6050 arduino sketch of sensor function". (), [Online]. Available: https://github.com/kriswiner/MPU6050. Accessed on: August, 13, 2023.

[70] J. H. Challis, "Quaternions as a solution to determining the angular kinematics of human movement", *BMC Biomedical Engineering*, vol. 2, 1 2020-12. DOI: 10.1186/S42490-020-00039-Z.

[71] R. H. Chowdhury, M. B. Reaz, M. A. B. M. Ali, A. A. Bakar, K. Chellappan, and T. G. Chang, "Surface electromyography signal processing and classification techniques", *Sensors (Basel, Switzerland)*, vol. 13, p. 12 431, 9 2013-09. DOI: 10.3390/S130912431.

[72] "Ambulatory measurement of shoulder and elbow kinematics through inertial and magnetic sensors", *Medical biological engineering computing*, vol. 46, pp. 169–178, 2008-02. DOI: 10.1007/S11517-007-0296-5.

[73] A. M. Valevicius, Q. A. Boser, E. B. Lavoie, *et al.*, "Characterization of normative hand movements during two functional upper limb tasks", *PLOS ONE*, vol. 13, 6 2018-06. DOI: 10.1371/JOURNAL.PONE.0199549.

[74] M. C. Lixandrão, P. R. Camargo, C. E. N. Scarpa, C. L. Prado-Medeiros, and T. F. Salvini, "Bilateral changes in 3-d scapular kinematics in individuals with chronic stroke", *Clinical biomechanics (Bristol, Avon)*, vol. 47, pp. 79–86, 2017-08. DOI: 10.1016/J.CLINBIOMECH.2017.06.002.

[75] WMA. "Wma declaration of helsinki – ethical principles for medical research involving human subjects – wma – the world medical association". (), [Online]. Available: https://www.wma.net/policies-post/wma-declaration-of-helsinki-ethical-principles-for-medical-research-involving-human-subjects/. Accessed on: September, 21, 2023.

[76] M. A. Murphy, S. Murphy, H. C. Persson, U. B. Bergström, and K. S. Sunnerhagen, "Kinematic analysis using 3d motion capture of drinking task in people with and without upper-extremity impairments", *Journal of visualized experiments : JoVE*, vol. 2018, 133 2018-03. DOI: 10.3791/57228.

APPENDIX A

SAMPLE CHARACTERIZATION QUESTIONNAIRE

Questionário de caracterização da amostra

O presente questionário pretende correlacionar os dados retirados com informações demográficas da população em estudo, e tirar conclusões mais completas acerca do estudo. Os dados recolhidos são anónimos e serão usados exclusivamente para a caracterização da amostra.

1. Idade:_____anos
2. Data de nascimento:_____/_____/_____
3. Sexo: ☐ Feminino ☐ Masculino
4. Altura:_____m
5. Peso:_____kg
6. Lado do corpo dominante: ☐ Esquerdo ☐ Direito
7. Prática de atividade física: ☐ Sim ☐ Não

Se sim, indique-nos:

- Frequência:_____semanal/mensal
- Desporto(s) que pratica: _____
- O desporto em questão envolve uma grande atividade do membro superior?

  (exemplos: jogos de raquetes; levantamento de pesos, etc.)

  ☐ Sim ☐ Não

Em nome de toda a equipa, o nosso agradecimento pela sua disponibilidade e colaboração

Figure A.1: Sample Characterization Questionnaire

APPENDIX B

FCT-UNL INFORMATIVE CONSENT

Consentimento para participação em estudo da área da saúde e engenharia biomédica

Tema: *Desenvolvimento de um dispositivo para análise cinemática e eletromiográfica do membro superior em contexto clínico.*

Área de estudo: Biomecânica; Processamento de Sinal Fisiológico

Eu,_____, declaro que me foi transmitido pelo investigador David Trindade, de forma adequada e inteligível, o objetivo da dissertação de mestrado e os procedimentos inerentes à participação neste estudo. Declaro que concordei em realizar o protocolo experimental explicado. Por fim, declaro que não sofro de qualquer patologia que afete o comportamento motor do membro superior.

Assinatura do Voluntário — Data (dd//mm//aaaa)

_____ _____

- Declaro ainda que, embora tendo concordado previamente em participar no estudo, poderei a qualquer momento durante o ensaio exigir a suspensão do mesmo e não permitir a utilização dos meus dados.

☐ Declaro verbalmente a retirada do consentimento previamente concedido para participação neste estudo.

Figure B.1: Informative Consent

APPENDIX C

PROTOTYPE

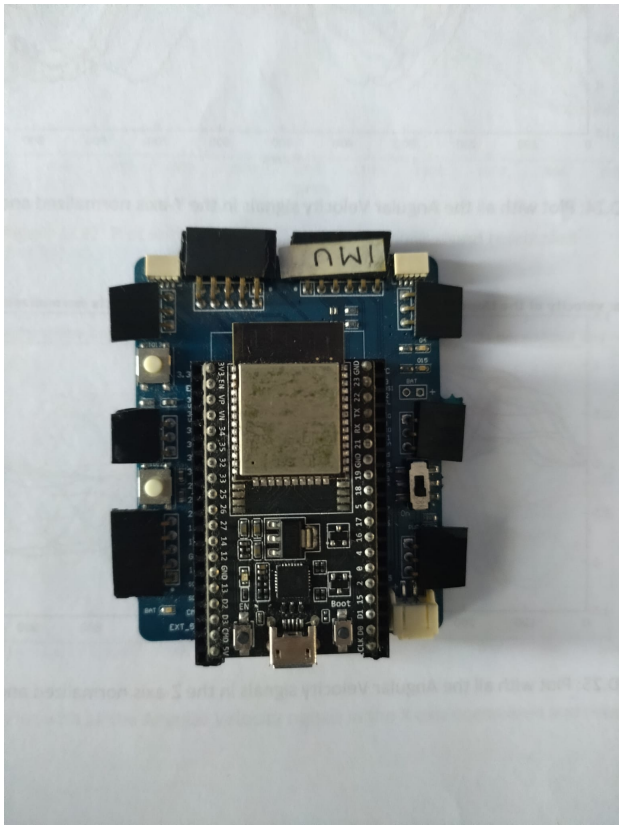

Figure C.1: Microcontroller used for the prototype

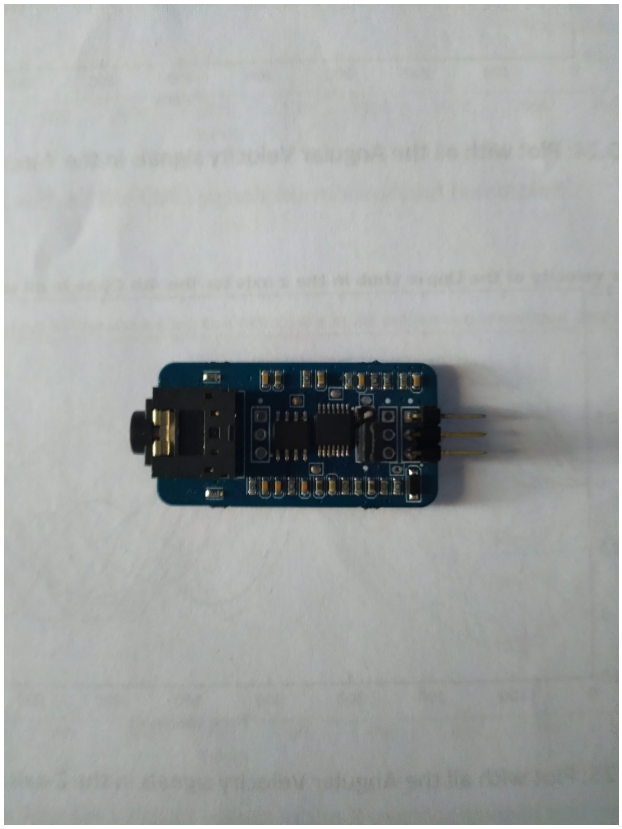

Figure C.2: EMG sensor used in the prototype

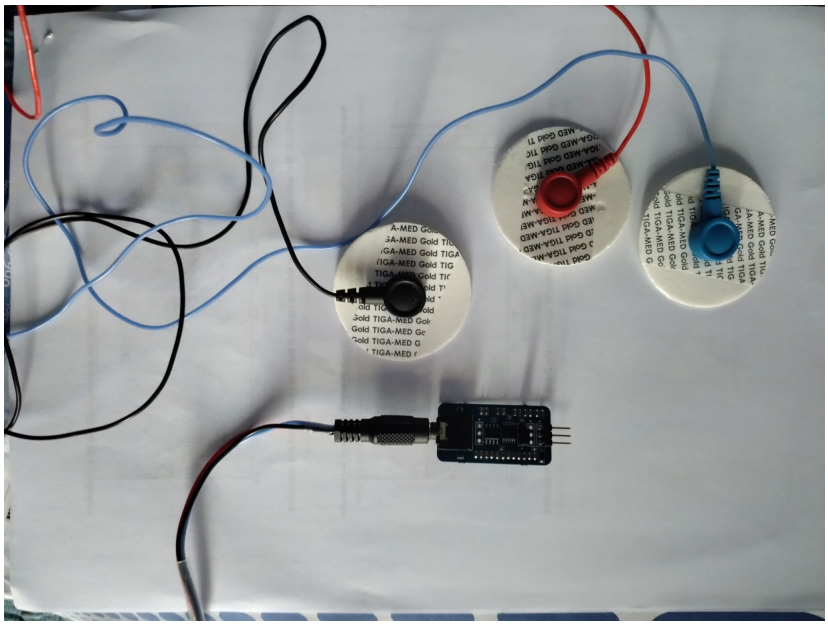

Figure C.3: EMG sensor with the cables with electrodes connected to it

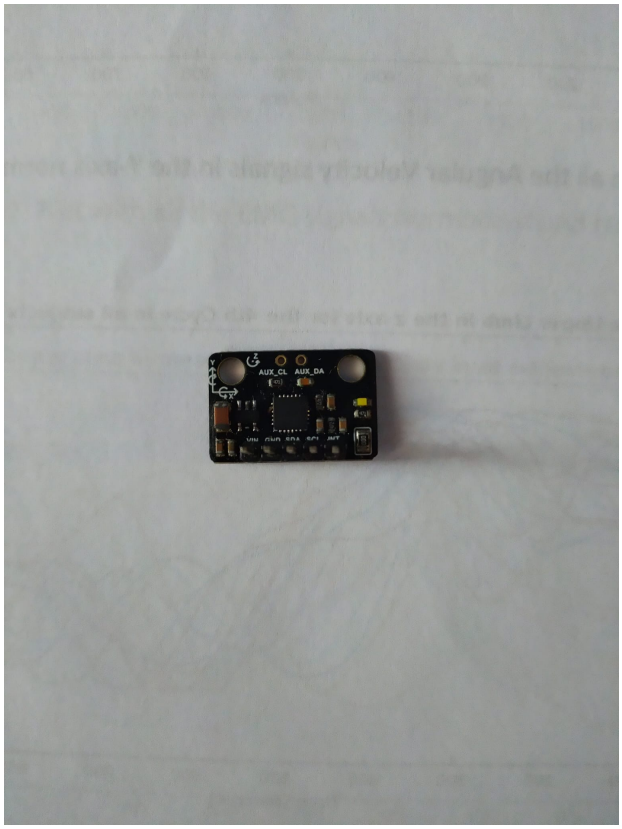

Figure C.4: MPU6050 used in the prototype

Appendix D

INTERFACE

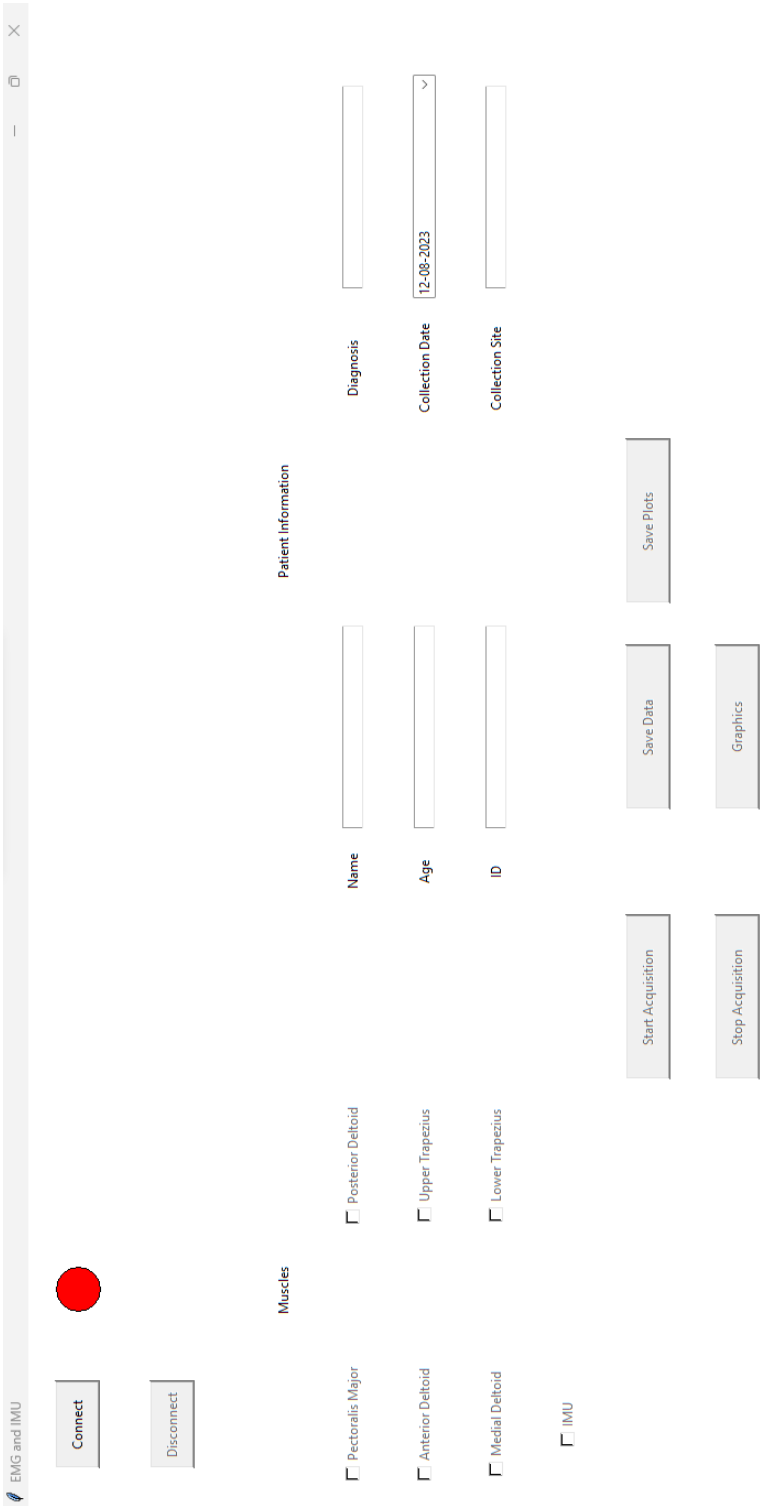

Figure D.1: Interface structure with the different components when opened

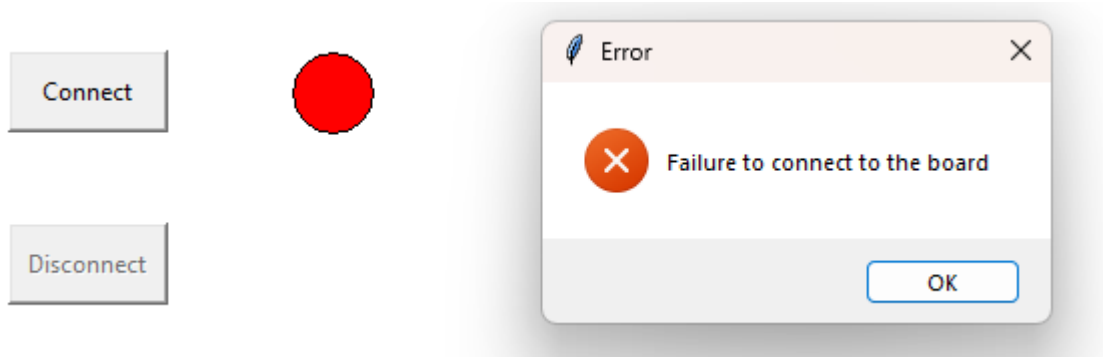

Figure D.2: Failed connection between the board and the Interface

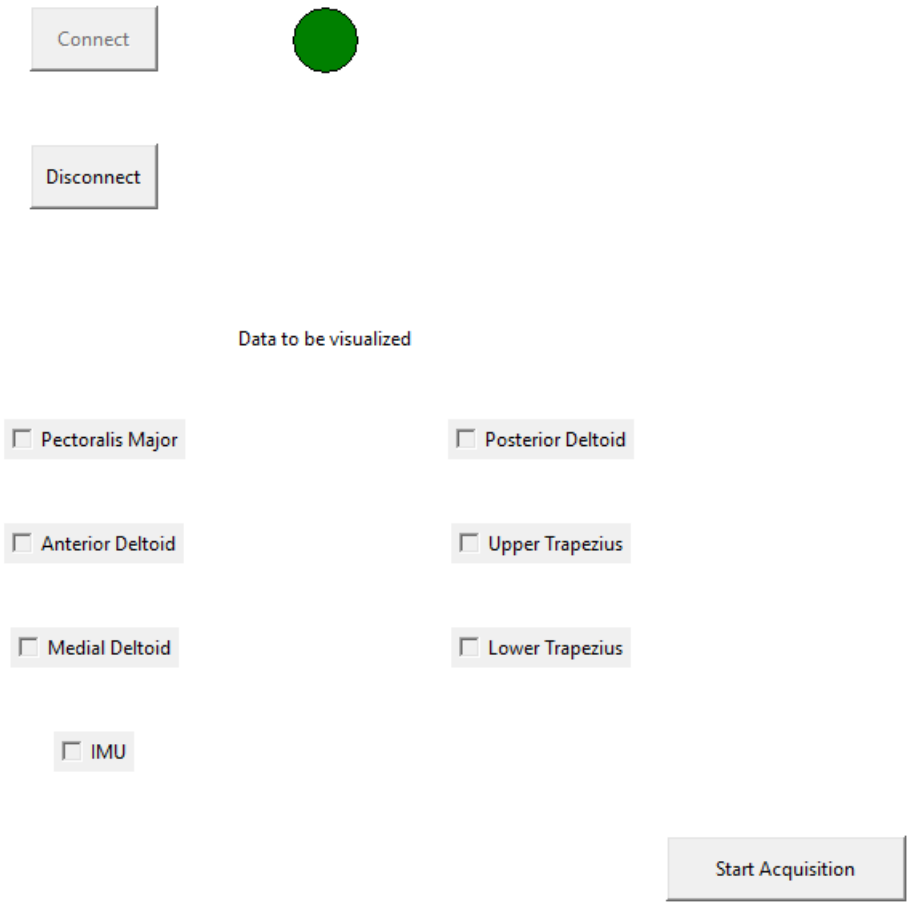

Figure D.3: Connection established between the Interface and the microcontroller

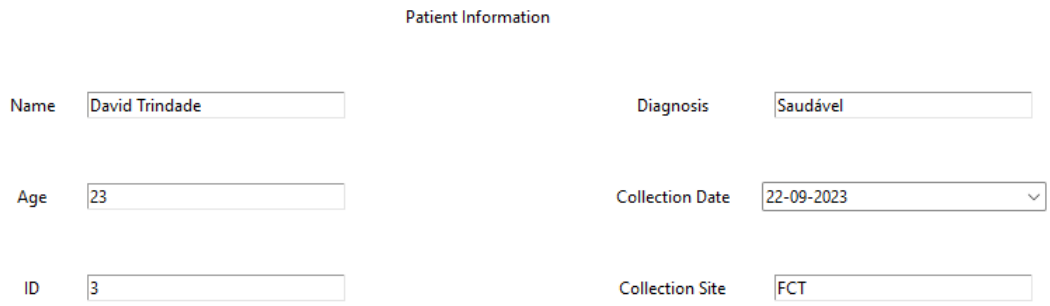

Figure D.4: Textboxes filled with information about the patient

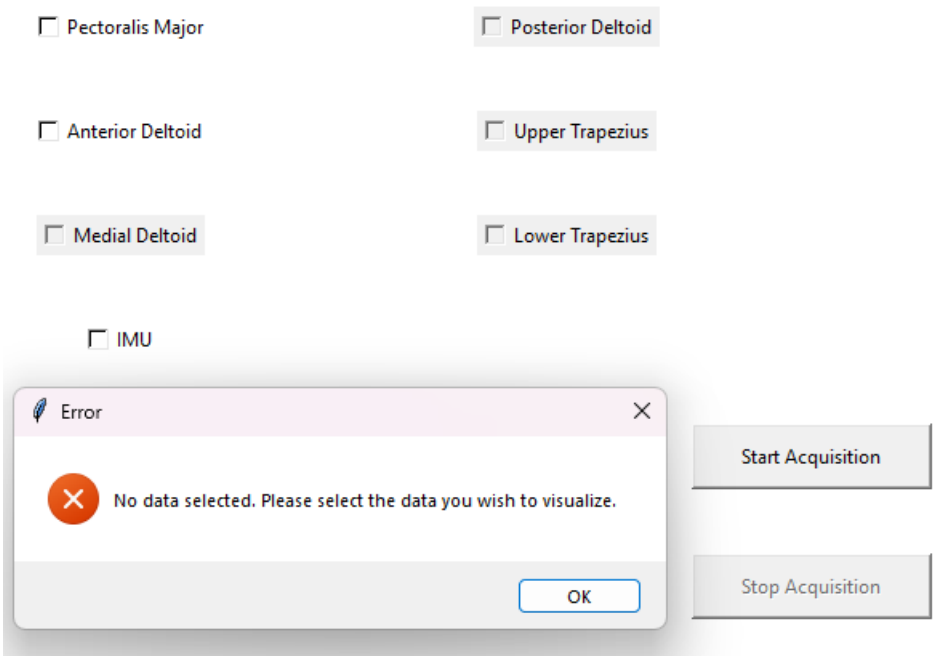

Figure D.5: Warning with the information that the acquisition couldn't start because there are none of the checkboxes is selected

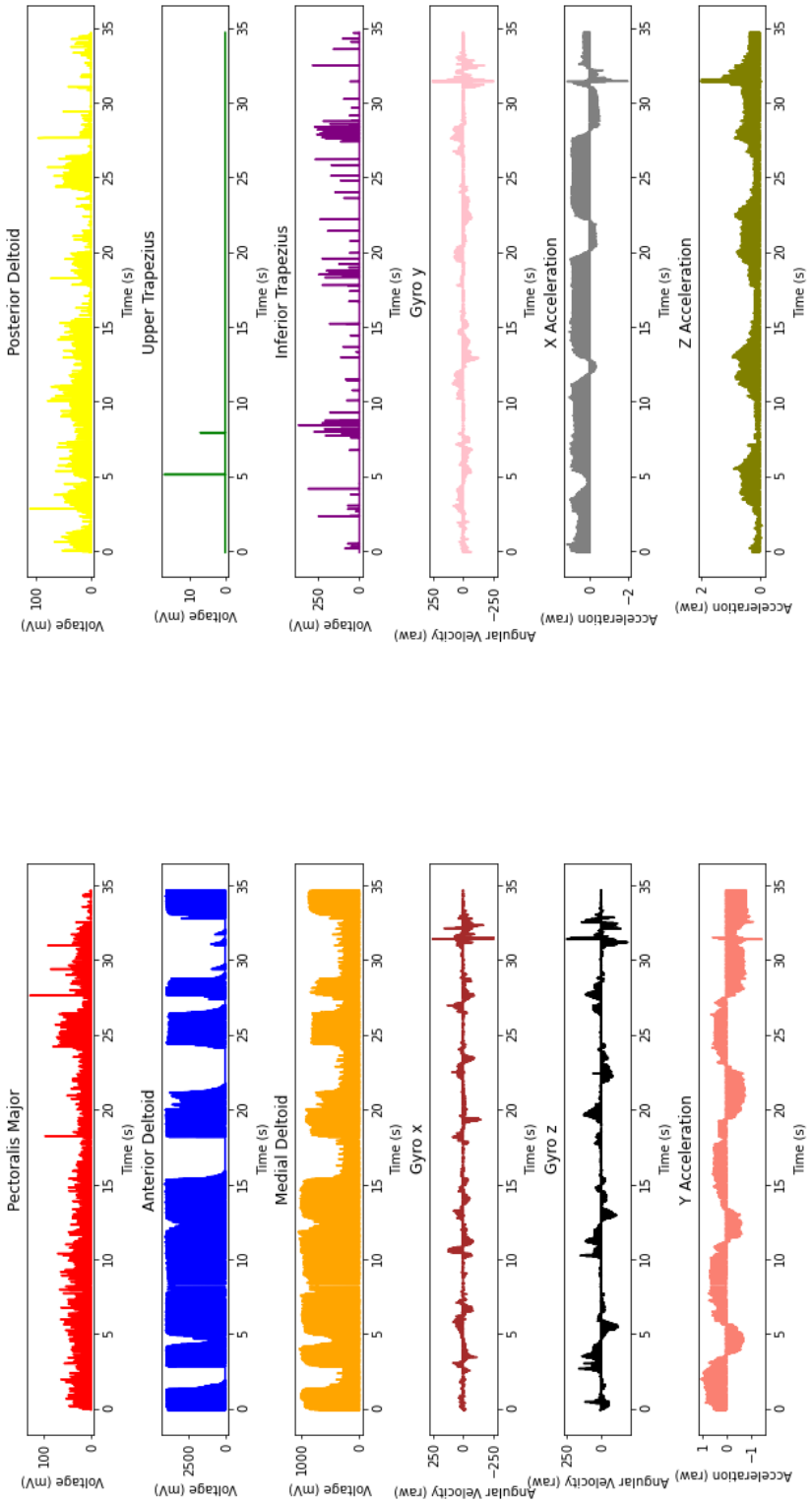

Figure D.6: All the different plots with the data acquired by the device

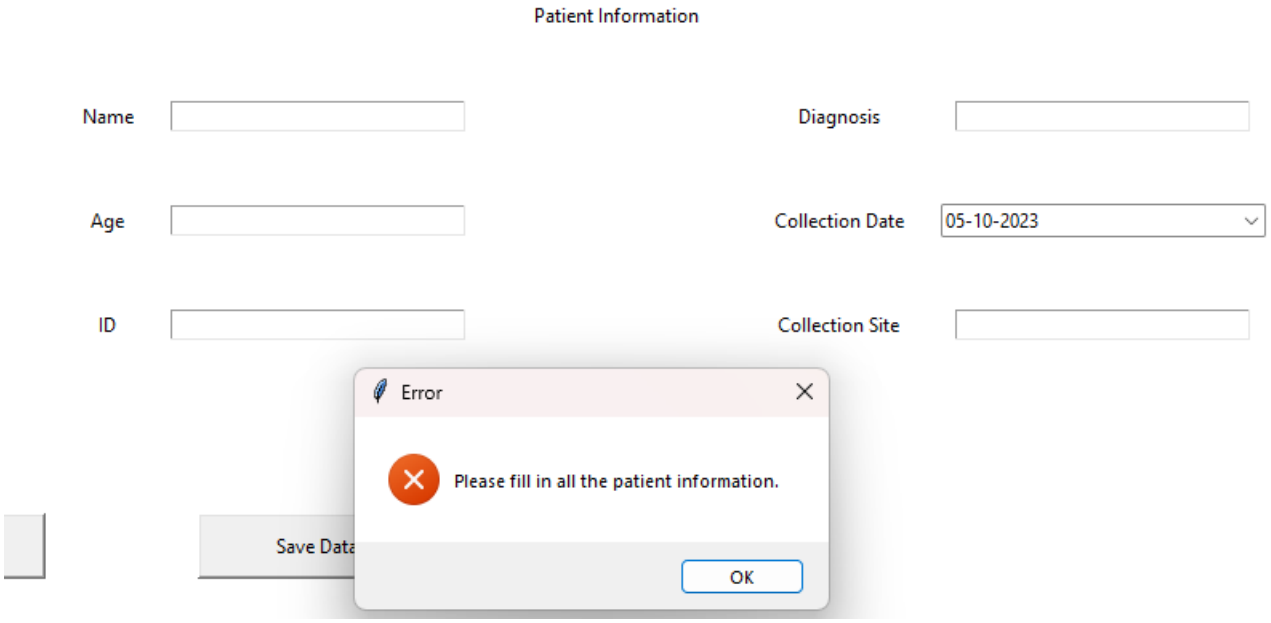

Figure D.7: Warning with the information that it was not possible to save the data into a CSV file or the PNG file with the plots because the text entry's weren't filled with the patient information

APPENDIX E

PLOTS OF THE DIFFERENT SIGNAL PROCESSING STEPS

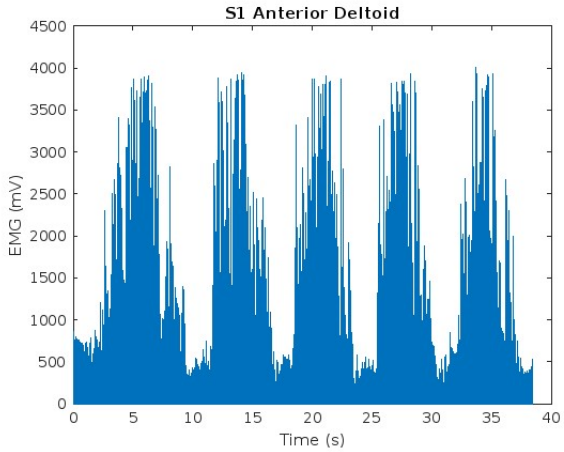

Figure E.1: EMG signal from a subject after a acquisition

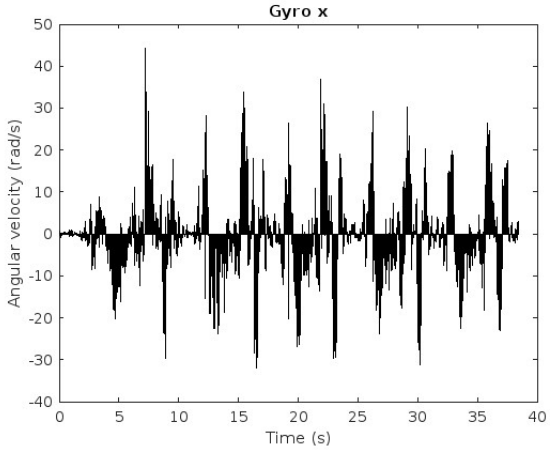

Figure E.2: Angular Velocity in the X-axis from a subject after a acquisition

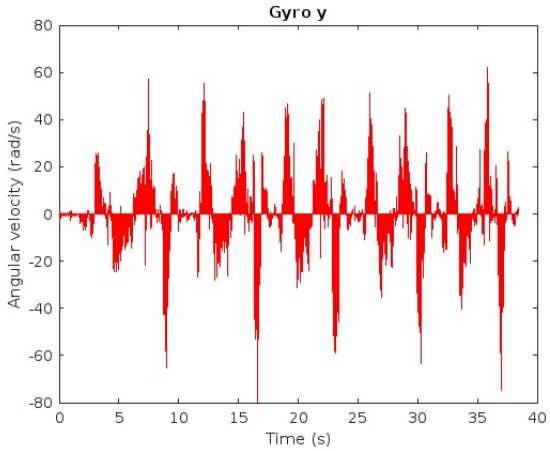

Figure E.3: Angular Velocity in the Y-axis from a subject after a acquisition

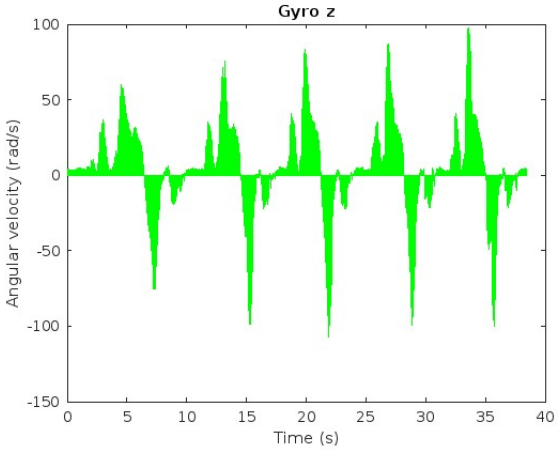

Figure E.4: Angular Velocity in the Z-axis from a subject after a acquisition

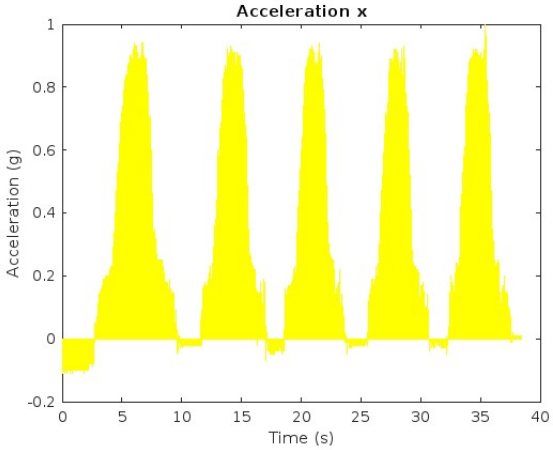

Figure E.5: Acceleration in the X-axis from a subject after a acquisition

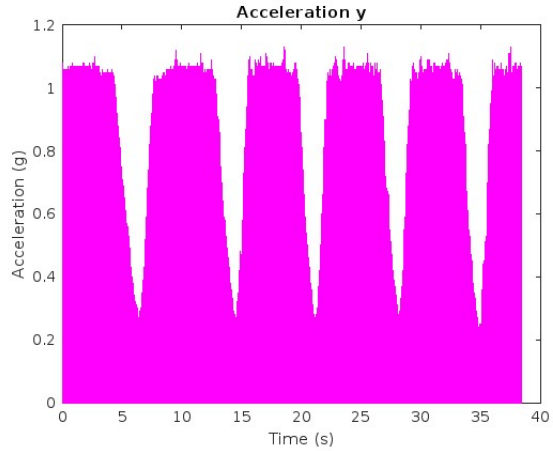

Figure E.6: Acceleration in the Y-axis from a subject after a acquisition

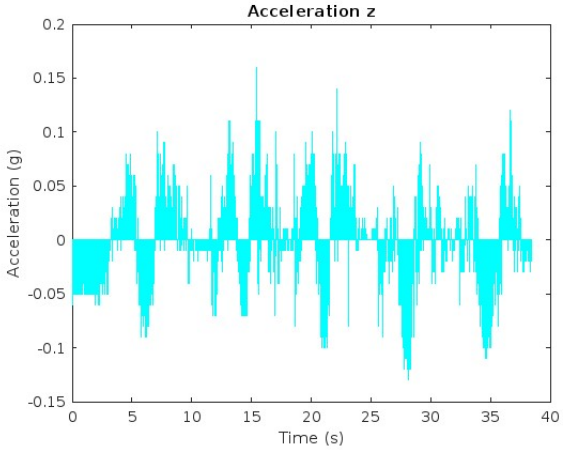

Figure E.7: Acceleration in the Z-axis from a subject after a acquisition

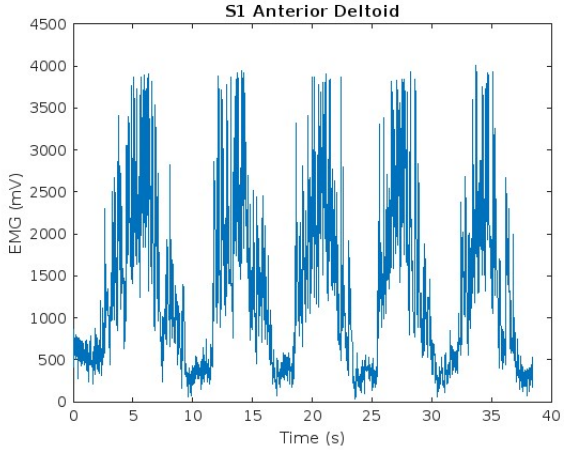

Figure E.8: EMG signal with the '0s' removed

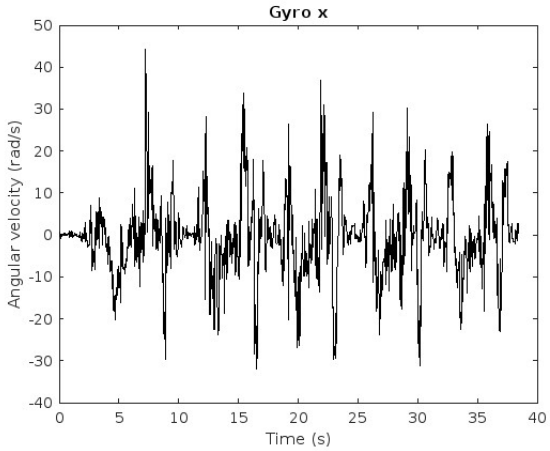

Figure E.9: Angular Velocity in the X-axis with the '0s' removed

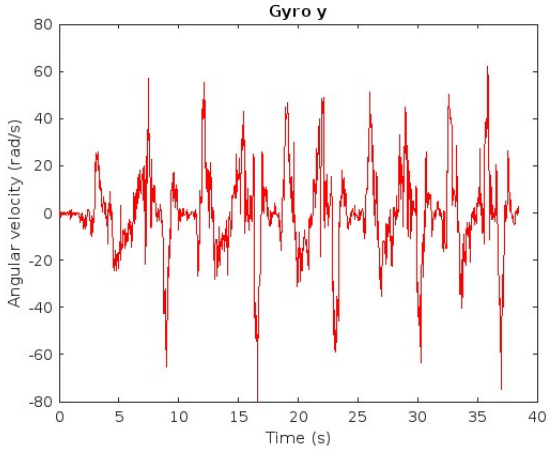

Figure E.10: Angular Velocity in the Y-axis with the '0s' removed

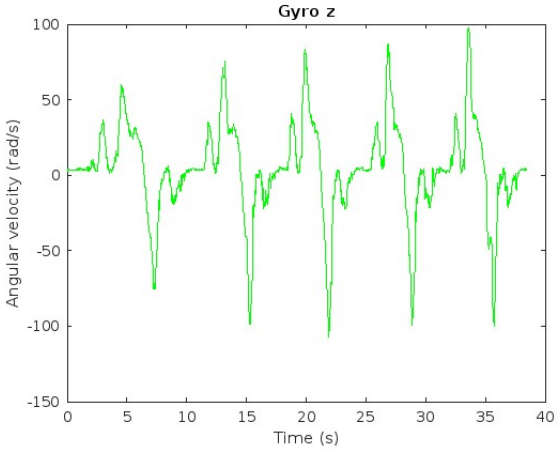

Figure E.11: Angular Velocity in the Z-axis with the '0s' removed

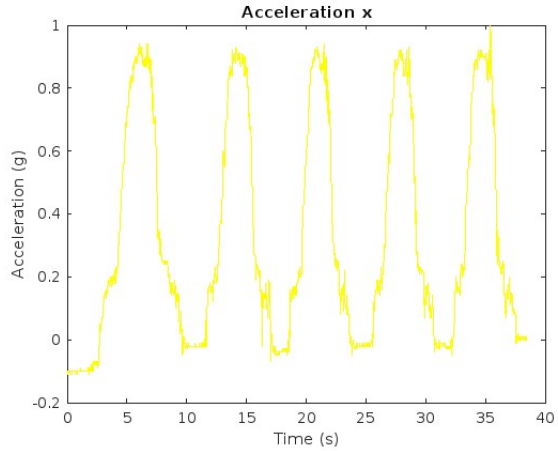

Figure E.12: Acceleration in the X-axis with the '0s' removed

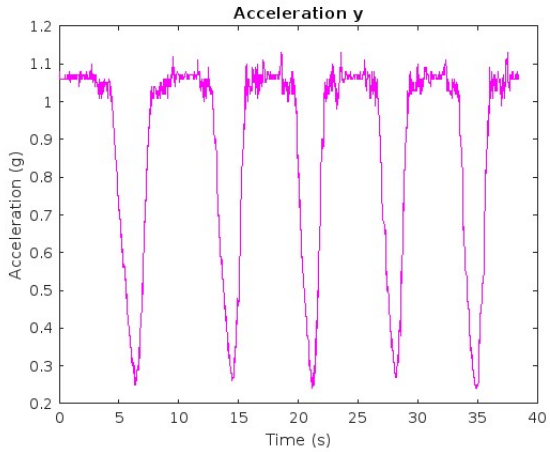

Figure E.13: Acceleration in the Y-axis with the '0s' removed

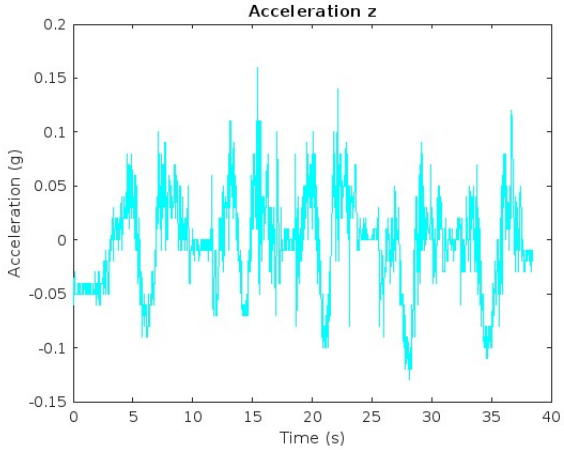

Figure E.14: Acceleration in the Z-axis with the '0s' removed

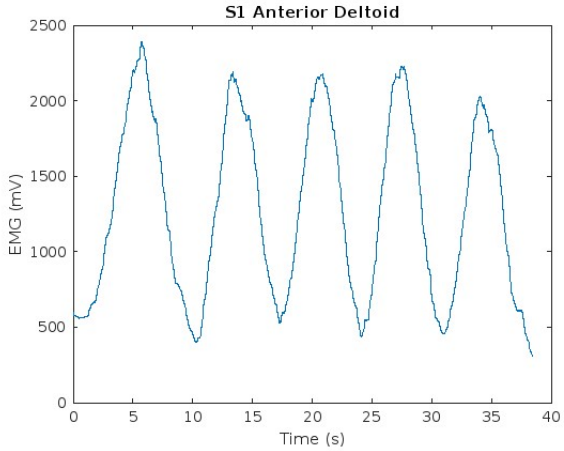

Figure E.15: EMG signal with the Moving Average Filter applied

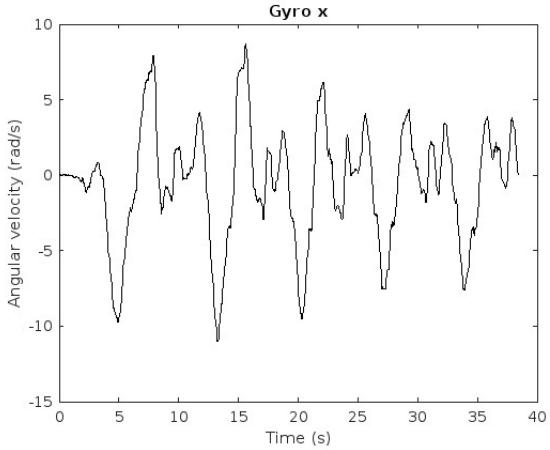

Figure E.16: Angular Velocity in the X-axis with the Moving Average Filter applied

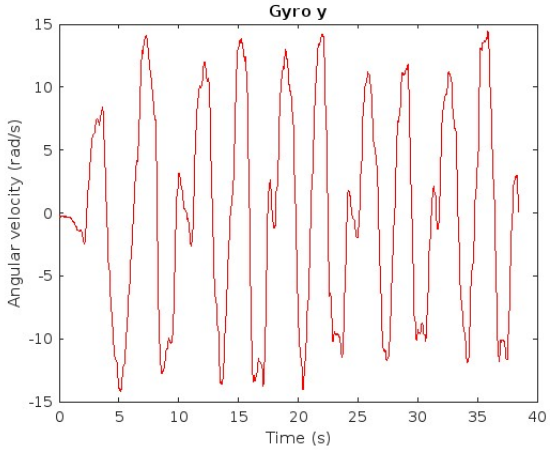

Figure E.17: Angular Velocity in the Y-axis with the Moving Average Filter applied

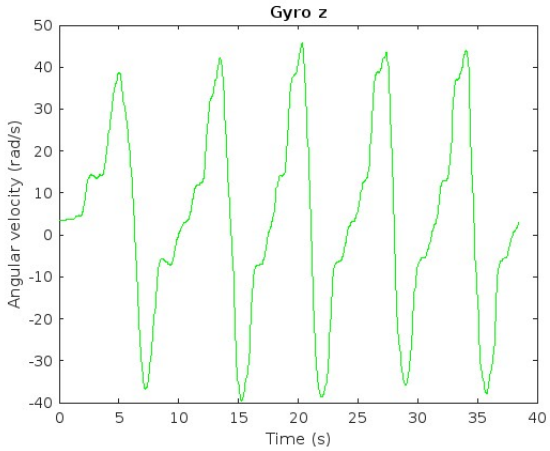

Figure E.18: Angular Velocity in the Z-axis with the Moving Average Filter applied

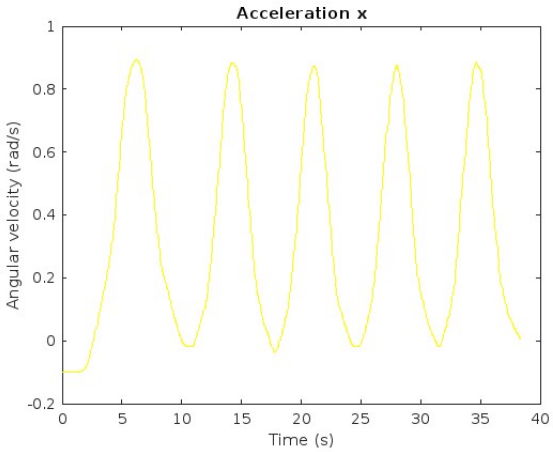

Figure E.19: Acceleration in the X-axis with the Moving Average Filter applied

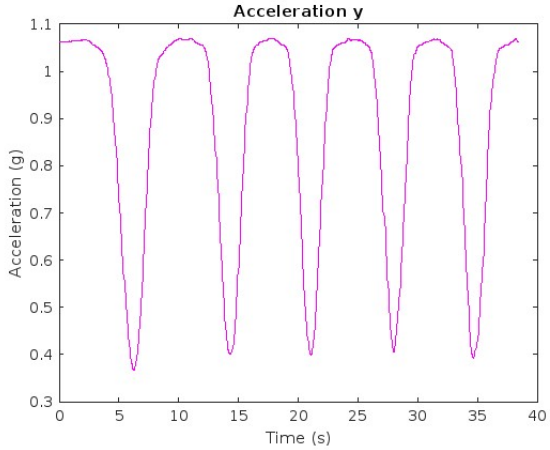

Figure E.20: Acceleration in the Y-axis with the Moving Average Filter applied

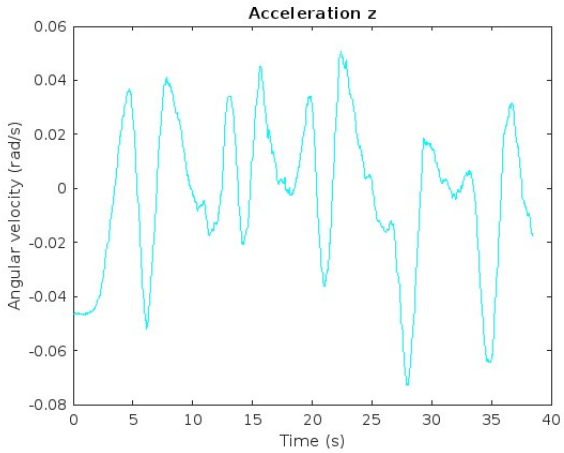

Figure E.21: Acceleration in the Z-axis with the Moving Average Filter applied

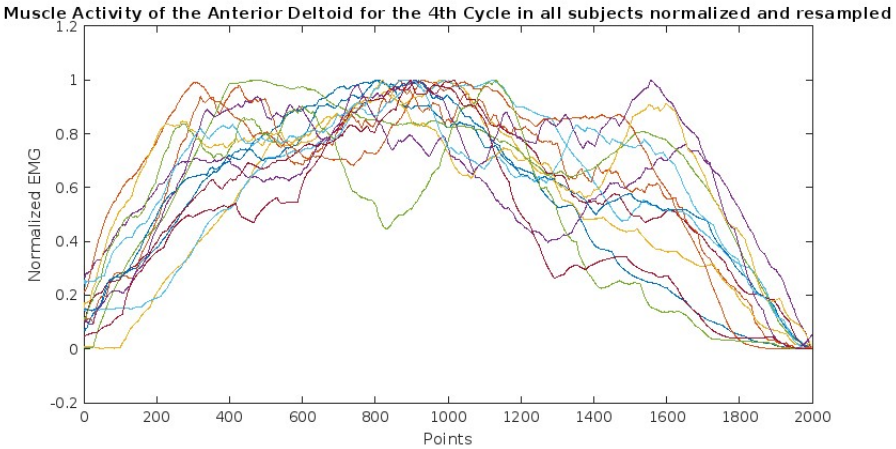

Figure E.22: Plot with all the EMG signals normalized and resampled

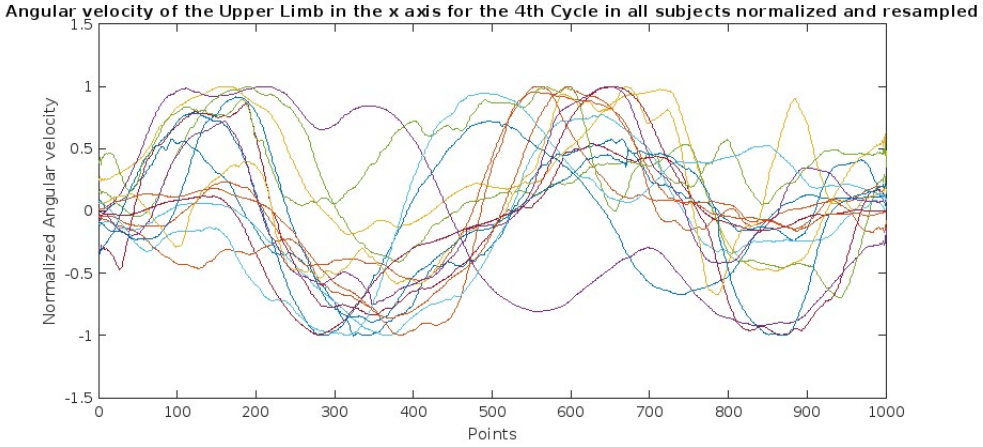

Figure E.23: Plot with all the Angular Velocity signals in the X-axis normalized and resampled

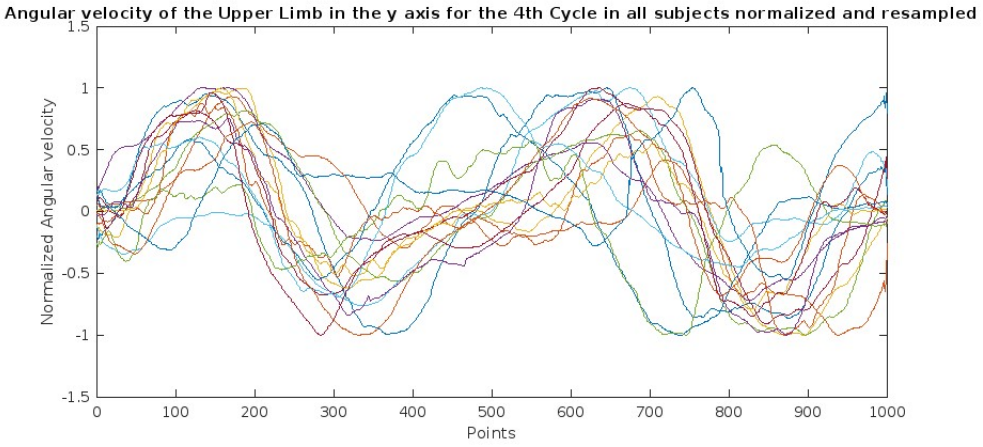

Figure E.24: Plot with all the Angular Velocity signals in the Y-axis normalized and resampled

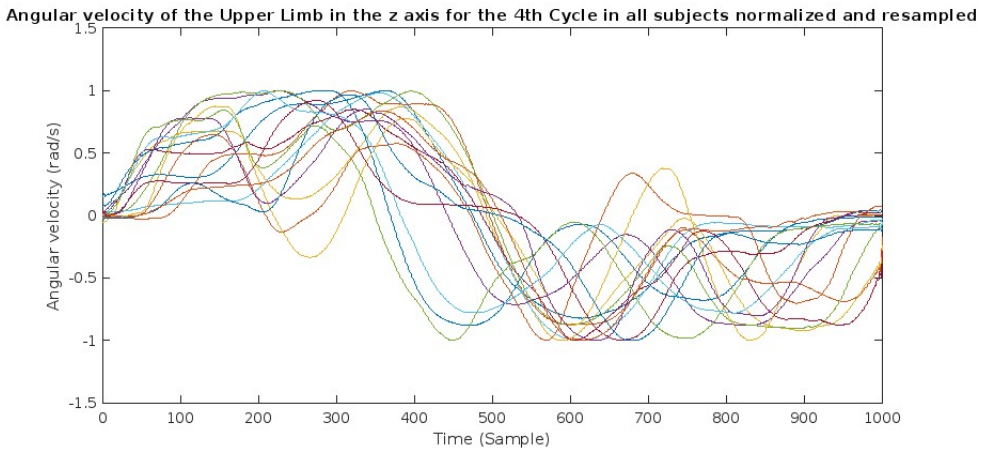

Figure E.25: Plot with all the Angular Velocity signals in the Z-axis normalized and resampled

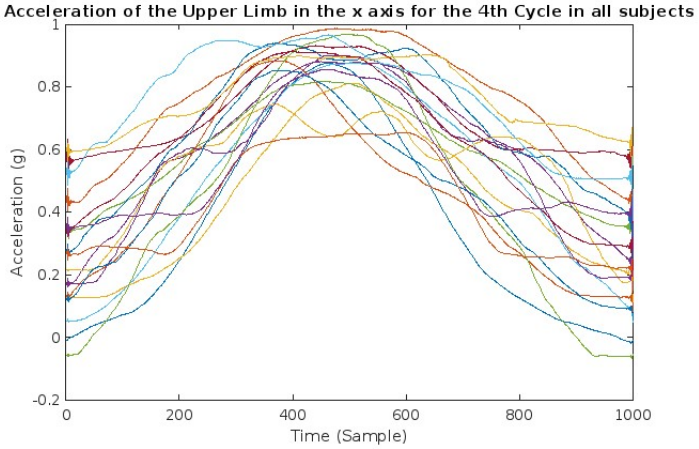

Figure E.26: Plot with all the Acceleration signals in the X-axis resampled

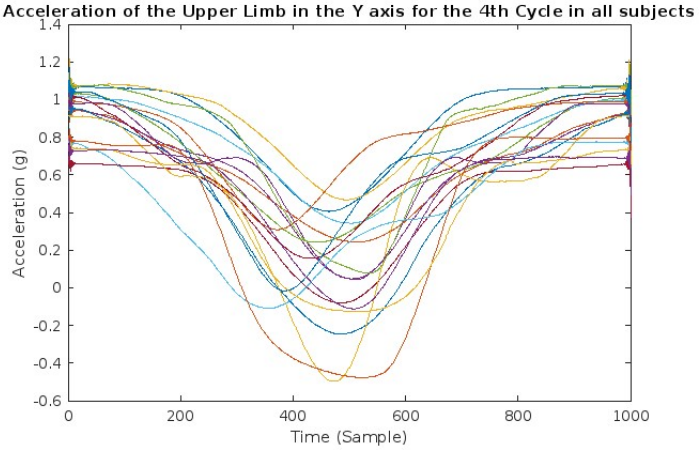

Figure E.27: Plot with all the Acceleration signals in the Y-axis resampled

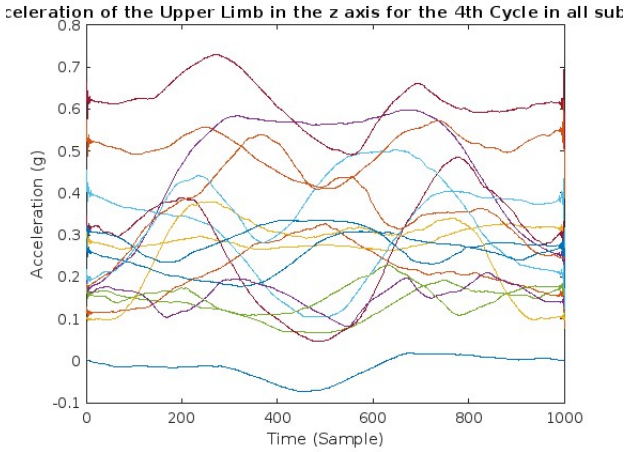

Figure E.28: Plot with all the Acceleration signals in the Z-axis resampled

APPENDIX F

PLOTS OF THE ANGULAR VELOCITY AND ACCELERATION RESULTS FOR THE LEFT HANDED PERSON

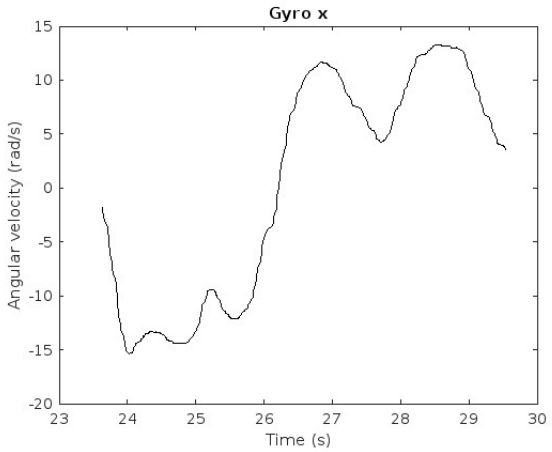

Figure F.1: Angular Velocity in the X axis of the left handed person

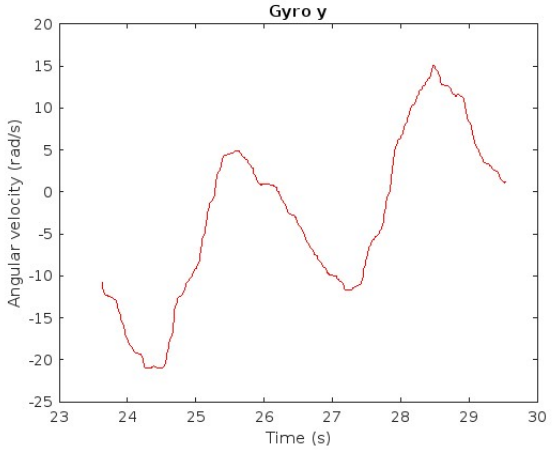

Figure F.2: Angular Velocity in the Y axis of the left handed person

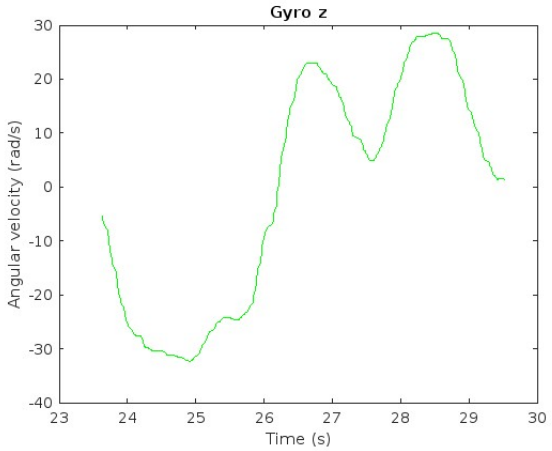

Figure F.3: Angular Velocity in the Z axis of the left handed person

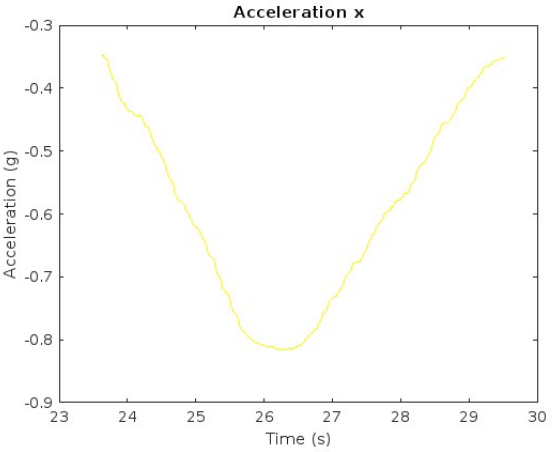

Figure F.4: Acceleration in the X axis of the left handed person